# Can oxygen isotopes in tree rings be used to detect stomatal responses to global change?

Imogen Carter<sup>1\*</sup>, Roel Brienen<sup>1</sup>, Manuel Gloor<sup>1</sup>

1: School of Geography, University of Leeds, United Kingdom, LS2 9JT

\*Correspondence: <a href="mailto:lkbs9646@leeds.ac.uk">lkbs9646@leeds.ac.uk</a>

### **Abstract**

- 2 Stomatal conductance (g<sub>s</sub>) regulates CO<sub>2</sub> and water fluxes of plants. Although experiments
- have shown that  $g_s$  decreases with elevated  $CO_2$ , it is unclear how  $g_s$  is responding *in-situ* to
- 4 long-term exposures to rising CO<sub>2</sub> and a changing climate. Tree ring isotope analysis provides
- 5 a unique method to assess tree ecophysiological responses to long-term exposures of slowly
- 6 changing environmental conditions. In particular, it has been suggested that changes in g<sub>s</sub> can
- potentially be inferred from tree ring stable oxygen isotope ratios ( $\delta^{18}O_{trc}$ ). Several studies
- have indeed used  $\delta^{18}O_{trc}$  trends to conclude that  $g_s$  has not significantly changed from
- 9 pre-industrial values. However, it remains unclear whether  $\delta^{18}O_{trc}$  is sufficiently sensitive to
- detect the magnitude of change in  $g_s$  expected due to  $CO_2$  increases and climatic changes.
- Here, we evaluate the sensitivity of  $\delta^{18}O_{trc}$  trends to  $CO_2$  and climate induced changes in  $g_s$ ,
- and to VPD and temperature increases since the beginning of the 20<sup>th</sup> century, using current
- theoretical models. We find that temporal changes in  $g_s$  only significantly affect  $\delta^{18}O_{trc}$  trends
- when the Péclet effect is present, and then only in dry climates. In contrast to the weak effects
- of  $g_s$  on  $\delta^{18}O_{trc}$  trends, we find that temporal increases in VPD and temperature, independent
- of changes in  $g_s$ , have far greater contributions to  $\delta^{18}O_{trc}$  trends. Thus, this increasingly
- popular method should be used with caution, because it is highly challenging to
- unambiguously attribute trends in  $\delta^{18}O_{trc}$  to changes in  $g_s$ . Despite current limitations, we
- recommend how future studies can address these challenges in efforts to detect long-term gs
- trends from tree ring records.
- 21 Key Words: intrinsic water-use efficiency; dual-isotope approach; stable isotope ratio;
- 22 Péclet effect; dendrochronology; stomatal conductance; Craig-Gordon-Dongmann
- 23 model

### Introduction

24

25 Plants are changing their functioning in response to rising atmospheric CO<sub>2</sub> concentrations and climatic changes, modulating the vegetation-climate system (Li, 2024). Of particular 26 interest are the ecophysiological responses of trees and forests to global change, as forests 27 cover about one third of Earth's land surface, and account for approximately 91% of the global 28 land carbon sink (Pan et al., 2024; FAO, 2020). Forests also play a significant role in the 29 30 hydrological cycle, for example by mediating atmospheric water transport over land, regulating surface water runoff, and recycling 40% of land-based precipitation via transpiration (Van der 31 Ent et al., 2010; Ellison et al., 2017). Free Air CO<sub>2</sub> Enrichment (FACE) studies (Bader et al., 32 2013; Walker et al., 2019; Norby et al., 2024), eddy covariance flux measurements (Keenan et 33 al., 2013; Fernández-Martínez et al., 2017), and tree ring stable carbon isotope ratio ( $\delta^{13}$ C) 34 studies (Saurer et al., 2014; Frank et al., 2015; van der Sleen et al., 2015) indicate physiological 35 changes in trees in response to rising CO<sub>2</sub> levels and climatic changes. Stomata regulate the 36 fluxes of CO<sub>2</sub> into, and water out of, the leaf, and thus, play a key role in these ecophysiological 37 changes. Consequently, it is important to understand how stomata are responding to global 38 change. 39 In controlled experiments, and rapid step increases in CO<sub>2</sub> concentrations (e.g. FACE studies), 40 it is generally observed that stomatal conductance (g<sub>s</sub>) decreases with rising CO<sub>2</sub> levels 41 (Ainsworth & Rogers, 2007; Gardner et al., 2022; Liang et al., 2023; Lammertsma et al., 2011; 42 Medlyn et al., 2001). Stomatal responses are further modulated by rising atmospheric 43 temperatures depending on water availability (Liang et al., 2023; Urban et al., 2017). Yet, 44 questions remain to what degree these experiments are representative of real-time responses 45 of trees to global change. Thus, there remains a need for in-situ evidence of stomatal 46 responses to long-term exposures to increasing CO<sub>2</sub> and climatic changes. 47

```
changes in leaf \delta^{18}O over time can reflect changes in g_s (Barbour et al., 2000). Leaf water \delta^{18}O
49
     is partially integrated within \delta^{18}O of tree ring cellulose - \delta^{18}O<sub>trc</sub> (Barbour & Farquhar, 2000),
50
     and changes in g_s may thus potentially be recorded in annual tree ring \delta^{18}O. Therefore, if g_s
51
     trends can be reliably inferred from \delta^{18}O_{trc} signals, tree ring \delta^{18}O analysis would be suitable to
52
     estimate the magnitude of in-situ past stomatal responses of trees to long-term exposures to
53
54
     increasing CO<sub>2</sub> and climatic changes.
     According to Farquhar et al. (1982), \delta^{13}C of leaf and cambial cellulose is related to the ratio of
55
     photosynthetic rate (A) to g<sub>s</sub>, which is termed intrinsic water use efficiency (iWUE). This ratio
56
     reflects the balance between the fluxes of carbon and water, with A related to primary
57
     production, and g<sub>s</sub> regulating the rate of transpiration (Osmond et al., 1980; Ehleringer et al.,
58
     1993). The majority of tree ring \delta^{13}C records indicate sustained increases in iWUE, and this
59
     has been attributed to rising CO<sub>2</sub> levels (Frank et al., 2015; Saurer et al., 2014; van der Sleen et
60
     al., 2015). To the extent that iWUE records and the Farquhar model can be trusted, and thus,
61
     that A/g<sub>s</sub> is increasing, it remains unclear whether this trend is caused by changes in A, or g<sub>s</sub>,
62
     or both.
63
     Scheidegger et al. (2000) proposed the 'dual-isotope approach' to constrain plant \delta^{13}C-derived
64
     changes in iWUE by using plant \delta^{18}O to infer changes in g<sub>s</sub>. This approach seeks to take
65
     advantage of independent information of A and g_s reflected in plant \delta^{18}O and \delta^{13}C records to
66
     determine the relative contributions of A and g<sub>s</sub> to iWUE trends. This is based on the
67
     assumption that g_s and plant \delta^{18}O are negatively related, when all other variables are held
68
     constant. Indeed, several studies report a robust negative relationship between g<sub>s</sub> and δ<sup>18</sup>O of
69
     leaf cellulose in controlled laboratory settings (Barbour et al., 2000; Grams et al., 2007), and
70
     in-situ (Sullivan&Welker, 2006; Moreno-Gutiérrez et al., 2011). The dual-isotope approach has
71
     since been applied to tree ring studies, using \delta^{18}O of tree ring cellulose to interpret iWUE
72
```

The stable oxygen isotope composition ( $\delta^{18}$ O) of leaf water is controlled in part by  $g_{s_i}$  and thus

trends (Nock *et al.*, 2011; Fajardo *et al.*, 2019; Siegwolf *et al.*, 2023). For a more detailed description of the dual-isotope approach, see the paper of Siegwolf *et al.*, (2023), which reviews more than 250 applications of the dual-isotope approach in plant physiological studies.

77

78

79

80

81

82

83

84

85

86

87

88

89

90

91

92

93

94

95

96

97

98

Two recent studies (Guerrieri et al., 2019, and Mathias & Thomas, 2021) have expanded on the tree ring dual-isotope approach by back-calculating <sup>18</sup>O-enrichment of leaf water above source water ( $\Delta^{18}O_{lw}$ ), using  $\delta^{18}O_{trc}$  measurements and estimates for historical variation of source water  $\delta^{18}O$  ( $\delta^{18}O_{sw}$ ). According to these studies, iWUE increases are largely due to increases in A, as they find that  $\Delta^{18}O_{lw}$ , and thus  $g_s$ , remained effectively unchanged. Mathias & Thomas (2021) conclude that g<sub>s</sub> has not changed in trees at 83% of the study sites, while Guerrieri et al. (2019) found that  $\delta^{18}O_{trc}$  increased in xeric sites, but did not change in trees from mesic sites. This led the authors to conclude that g<sub>s</sub> reductions were restricted to species in moisture-limited conditions. However, the methods employed in these studies were criticised on several grounds by Lin et al. (2022). First, longer-term temporal  $\delta^{18}O_{sw}$  trends at each site were calculated using a spatially explicit model of precipitation  $\delta^{18}$ O, which poorly estimated precipitation  $\delta^{18}$ O trends across time. Secondly, background noise in  $\delta^{18}$ O signals due to interannual climatic variability was not appropriately considered. This is a significant source of error because this application of the dual-isotope approach requires other factors that influence  $\delta^{18}$ O (e.g. inter-annual variability of relative humidity) to be constant, in order to infer that changes in  $\delta^{18}$ O are caused by changes to  $g_s$  (Roden & Siegwolf, 2012). Thirdly, the studies assumed a uniform negative  $g_s$ - $\delta^{18}$ O relationship across all species, which relies on the assumption that the Péclet effect is of similar magnitude for all species. However, the Péclet effect may not be the same for all species (Barbour et al., 2021; Song et al., 2013). Considering this, Lin et al. (2022) demonstrate that changes in g<sub>s</sub> in the order of 0.1 mol m<sup>-2</sup> s<sup>-1</sup> are on the limit of detectability (0.3%) in  $\delta^{18}O_{trc}$  trends when the Péclet effect is absent, and changes in  $\delta^{18}O_{trc}$  may be even smaller if the Péclet effect varies with transpiration rate. This

implies that  $g_s$  trends may not always be detectable in  $\delta^{18}O_{trc}$  signals. Additionally, theory 99 suggests that changes in  $g_s$  have their strongest effect on  $\delta^{18}O$  in dry conditions (Roden & 100 Siegwolf, 2012). Thus, it may be that decreases in  $g_s$  are simply only detectable in  $\delta^{18}O_{trc}$ 101 102 series at water-limited sites, and not in wet sites, potentially leading to false impressions that g<sub>s</sub> did not change at these mesic sites. 103 In summary, it remains unclear what conditions are required for changes in g<sub>s</sub> due to CO<sub>2</sub> and 104 anthropogenic climate change to be detectable in  $\delta^{18}O_{trc}$  trends. There is emerging 105 experimental research into the sensitivity of cellulose  $\delta^{18}$ O to the effects of rising CO<sub>2</sub> 106 concentrations on g<sub>s</sub> for some grass, legume and herb species (Morgner et al., 2024) and for 107 trees e.g. Pinus mugo and Larix decidua (Streit et al., 2014). Existing research indicates that 108 increasing temperatures and VPD significantly increase  $\delta^{18}O_{trc}$  by driving  $^{18}O$ -enrichment at 109 the evaporating site of the leaf for trees, independent of changes to g<sub>s</sub> (Kahmen et al., 2011; 110 Cheesman & Cernusak, 2016; Streit et al., 2014). Thus, it remains important to quantify the 111 relative contributions of temporal changes in climate, and of g<sub>s</sub> responses to CO<sub>2</sub> and climatic 112 changes, to  $\delta^{18}O_{trc}$  trends to determine whether changes in  $g_s$  due to anthropogenic global 113 change can be reliably inferred from  $\delta^{18}O_{trc}$  signals. 114 The aim of this article is to determine the sensitivity of  $\delta^{18}O_{trc}$  trends to changes in  $g_s$  due to 115 anthropogenic CO<sub>2</sub> emissions and associated climatic changes. We disentangle the sensitivity 116 of  $\Delta^{18}O_{lw}$  and  $\delta^{18}O_{trc}$  trends to simultaneous increases in  $CO_2$  concentrations, atmospheric 117 temperature and VPD over the past 150 years using standard mechanistic models of oxygen 118 isotopic composition in plant tissues. We do this for an idealised mature tree growing in a 119 Northern latitude temperate climate using various physiological and environmental 120 assumptions to determine under what conditions  $\delta^{18}O_{trc}$  trends can be used to detect a 121 change in g<sub>s</sub>. We discuss the implications of our results in view of the conclusions of recent 122 studies that have used  $\delta^{18}O_{trc}$  trends to infer how  $g_s$  has changed in response to rising  $CO_2$ 123

- levels. Ultimately, we evaluate whether current applications of tree ring  $\delta^{18}$ O analysis can
- determine how  $g_s$  has changed since the beginning of the  $20^{th}$  century.
- The next section describes the existing theory for tree stable oxygen isotope models. Then, we
- describe the modelling approach employed to address the aims of this article, followed by the
- results and discussion sections.

## Theory and illustration of mechanisms

According to current understanding, tree ring cellulose  $\delta^{18}O$  ( $\delta^{18}O_{trc}$ ) is a mixed signal coming from variation in  $\delta^{18}O$  of the source water and evaporative enrichment of that source water signal in the leaf (Figure 1).

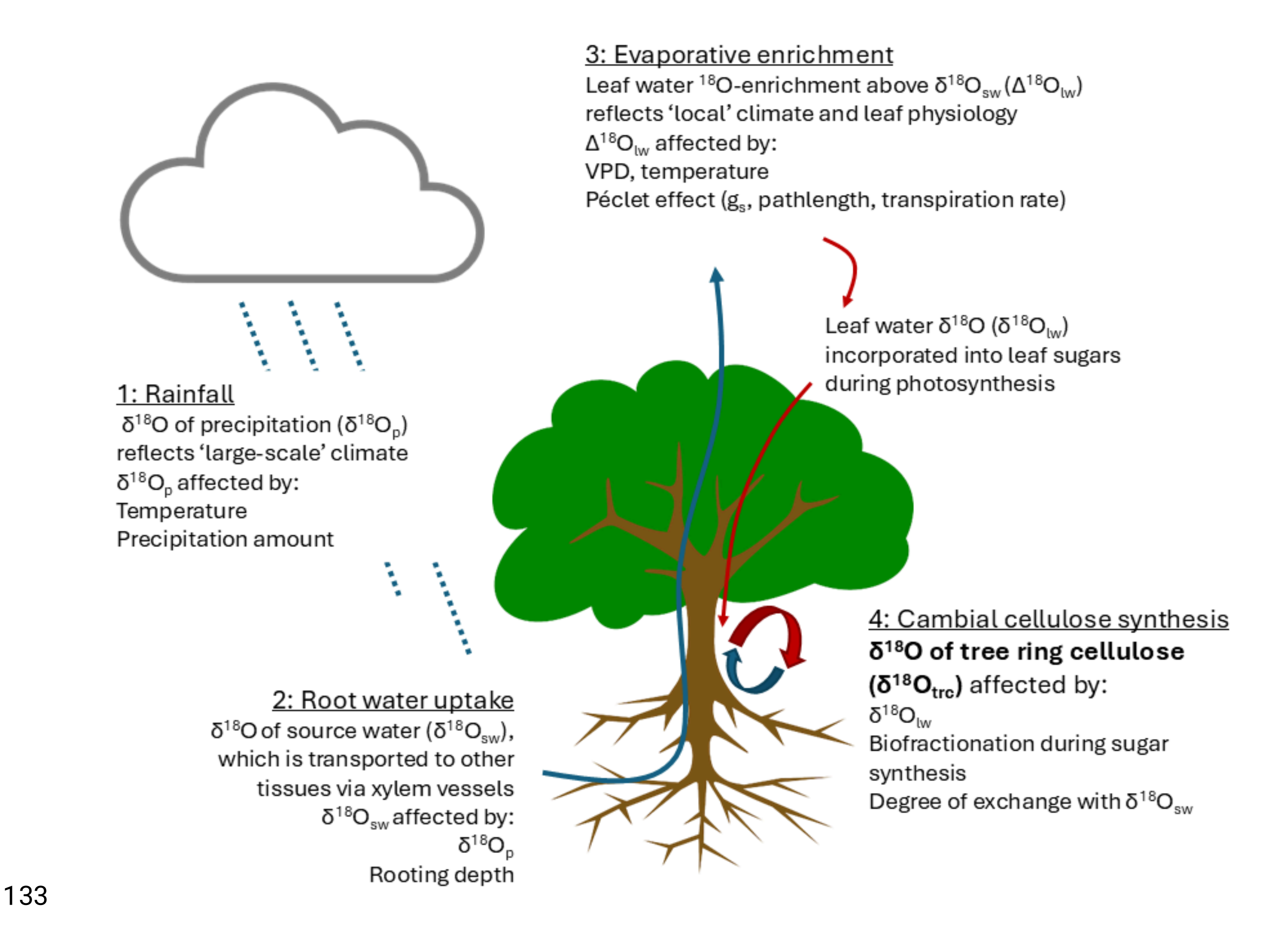


**Figure 1** The transfer of oxygen isotope signals from rainwater to tree ring cellulose.  $\delta^{18}$ O of precipitation (1) contains an imprint of climate (temperature, precipitation amount and large-scale rainout processes). These signals are transferred from precipitation to (2) soil, xylem and leaf water, and then altered by leaf evaporative enrichment (3), biofractionations, and exchange with xylem water during cellulose synthesis (4).

**Table 1** Abbreviations of all parameters used in the oxygen isotope models

Abbreviation	Definition (unit)
δ <sup>18</sup> Ο	Deviation in the stable 18-oxygen and 16-oxygen isotope ratio between a sample
	and a standard reference (‰)
$\delta^{18}O_{sw}$	δ <sup>18</sup> O of source water (‰)
$\delta^{18}O_{wv}$	$\delta^{18}$ O of atmospheric water vapour (%)
$\delta^{18}O_{es}$	$\delta^{18}$ O of water at evaporating site of leaf (‰)
$\Delta^{18}O_{es}$	$\delta^{18}$ O enrichment of water at evaporating site above $\delta^{18}$ O $_{\mathrm{sw}}$ (%)
$\delta^{18}O_{lw}$	$\delta^{18}O$ of bulk leaf water (%)
$\Delta^{18}O_{lw}$	$\delta^{18}$ O enrichment of bulk leaf water above $\delta^{18}$ O <sub>sw</sub> (%)
$\delta^{18}O_{trc}$	$\delta^{18}O$ of tree ring cellulose (%)
ε <sub>k</sub>	Kinetic fractionation of water during diffusion through the stomata and leaf
	boundary layer (‰)
£*	Equilibrium fractionation between liquid water and vapour during evaporation (‰)
ε <sub>bio</sub>	Biochemical fractionation of cellulose synthesis (%)
$e_a$	Atmospheric vapour pressure (kPa)
$e_i$	Leaf internal vapour pressure (kPa)
VPD	Leaf-to-air vapour pressure deficit = $(e_i - e_a)$ (kPa)
Р	Atmospheric pressure (kPa)
$g_{_{\mathcal{S}}}$	Stomatal conductance (mol m <sup>-2</sup> s <sup>-1</sup> )

$g_b$	Boundary layer conductance (mol m <sup>-2</sup> s <sup>-1</sup> )
p <sub>ex</sub>	Proportion of oxygen in cellulose exchanged with medium water during cellulose synthesis
$p_{x}$	Proportion of medium water at site of cellulose synthesis that is source water
E	Transpiration rate (mol m <sup>-2</sup> s <sup>-1</sup> )
L	Effective pathlength (m)
С	Molar density of water (mol m <sup>-3</sup> )
D	Molecular diffusivity of water (m <sup>2</sup> s <sup>-1</sup> )
Ю	Péclet number

The plant source water  $\delta^{18}O$  ( $\delta^{18}O_{sw}$ ) variation is determined by rainfall  $\delta^{18}O$ , which is controlled by the movement of heavy and light water through the large-scale hydrological cycle. Rainwater  $\delta^{18}O$  increases with air temperature during condensation, decreases with increasing precipitation intensity, and decreases as the path length of water vapour transport increases (i.e. towards higher latitudes and altitudes, and further inland) due to Rayleigh distillation effects (Dansgaard, 1964; Rozanski *et al.*, 1992). Plant source water  $\delta^{18}O$  largely reflects precipitation  $\delta^{18}O$  but this may vary depending on root water uptake from different soil depths. For example, groundwater  $\delta^{18}O$  can vary significantly from precipitation  $\delta^{18}O$ , and kinetic fractionation during evaporation at the soil surface and within the soil pores causes  $\delta^{18}O$ -enrichment of soil water relative to rainwater (Ehleringer & Dawson, 1992; Sprenger *et al.*, 2017). Xylem water  $\delta^{18}O$  is equal to  $\delta^{18}O_{sw}$ , because no fractionation is assumed during water uptake by roots (Allison *et al.*,1984; Dawson & Ehleringer, 1991).

Water is transported through the tree to the stomatal opening of the leaf via the transpiration stream. The  $\delta^{18}$ O of water at the evaporating site of the leaf ( $\delta^{18}$ O<sub>es</sub>) increases because 'light'  $H_2^{16}$ O evaporates more readily than 'heavy'  $H_2^{18}$ O. Enrichment of <sup>18</sup>O at the evaporating site of the leaf is modelled by the Craig-Gordon-Dongmann (CGD) equation (Craig & Gordon, 1965; Dongmann *et al.*, 1974; Farquhar&Lloyd, 1993):

158 [1] 
$$\delta^{18}O_{es} = (\delta^{18}O_{sw} + \epsilon_k) \left( \frac{e_i - e_a}{e_i} \right) + \epsilon * + \delta^{18}O_{wv} \left( \frac{e_a}{e_i} \right)$$

- 159 Where  $\varepsilon_k$  is the kinetic fractionation of water during diffusion through the stomata and leaf
- boundary layer (%), ei is the internal vapour pressure of the leaf at saturation (kPa) (c.f. Eqn.
- 161 SI.3.1), ea is atmospheric vapour pressure (kPa), e\* is the equilibrium fraction between liquid
- water and vapour during evaporation from the mesophyll (%), and  $\delta^{18}O_{wv}$  is  $\delta^{18}O$  of
- 163 atmospheric water vapour (%).
- 164 Kinetic fractionation is typically in the range of 28-32‰, and occurs during diffusion of water
- through the stomata and leaf boundary layer, and is thus related to stomatal conductance (g<sub>s</sub>)
- and boundary layer conductance (g<sub>b</sub>), according to (Farquhar *et al.*, 1998; Barbour, 2007):

167 [2] 
$$\varepsilon_{\mathbf{k}} = \frac{32g_{\mathbf{s}}^{-1} + 21g_{\mathbf{b}}^{-1}}{g_{\mathbf{s}}^{-1} + g_{\mathbf{b}}^{-1}}$$

- 168 Equilibrium fractionation is temperature-dependent and typically in the range of 9-10‰, and
- occurs during evaporation of water from the site of evaporation in the leaf (Bottinga & Craig,
- 170 1969):

171 [3] 
$$\varepsilon^* = 2.644 - \left(3.206 * \frac{10^3}{T_{leaf}}\right) + \left(1.534 * \frac{10^6}{T_{leaf}^2}\right)$$

where T<sub>leaf</sub> is leaf temperature (Kelvin).

To control for variation in  $\delta^{18}O_{sw}$ ,  $^{18}O$ -enrichment of water at the evaporating site can be expressed above  $\delta^{18}O_{sw}$  (i.e.  $\Delta^{18}O_{es} = \delta^{18}O_{es} - \delta^{18}O_{sw}$ ), and can be approximated as (Barbour et al., 2004):

176 [4] 
$$\Delta^{18}O_{es} \approx \epsilon^* + \epsilon_k \left(1 - \frac{e_a}{e_i}\right)$$
,

- 177 assuming  $\delta^{18}O_{sw} = \delta^{18}O_{wv}$ .
- 178 The CGD model shows that  $\Delta^{18}O_{es}$  increases with increasing evaporative demand, i.e.
- increasing leaf-to-air vapour pressure deficit VPD=(e<sub>i</sub> e<sub>a</sub>), or decreasing relative humidity –
- 180 RH ( $e_a/e_i$ ). Under 100% RH ( $e_a/e_i$  =1), the contribution of  $\epsilon_k$  to  $\Delta^{18}O_{es}$  is 0, and  $\Delta^{18}O_{es}$  is thus
- 181 equal to  $\varepsilon_*$ . Under decreasing RH, the contributions of  $\varepsilon_k$  to  $\Delta^{18}O_{es}$  increases, leading to higher
- 182  $\Delta^{18}O_{es}$ .
- 183 For applications of the CGD model across large temporal and spatial scales (e.g.  $\delta^{18}$ O signals
- integrated into tree ring material) it is usually assumed that source water and atmospheric
- water vapour are equal and in steady-state isotopic equilibrium, i.e.  $\delta^{18}O_{sw} = \delta^{18}O_{wv}$  (Cernusak
- 186 et al., 2016). This steady-state assumption is not necessarily correct, but non-steady state
- models are highly complex and do not significantly improve modelling accuracy compared to
- the steady-state assumption (Cernusak *et al.*, 2016). Thus, for the purpose of this study we
- only use the model with this assumption.
- The first leaf isotope models assumed that there is no compartmentalisation of water in the
- leaf, i.e. bulk leaf water  $\delta^{18}$ O is the same as  $\delta^{18}$ O at the site of evaporation ( $\delta^{18}$ O<sub>lw</sub> =  $\delta^{18}$ O<sub>es</sub>).
- However, multiple studies have demonstrated that leaf and cellulose  $\delta^{18}$ O are a mixture of
- 193  $\delta^{18}O_{es}$ , and the unenriched  $\delta^{18}O$  of water in the transpiration stream i.e.  $\delta^{18}O_{sw}$  (Walker *et al.*,
- 194 1989; Flanagan et al., 1994). To account for this, Farquhar&Lloyd (1993) incorporated a 'Péclet

effect' into the CGD model by modelling  $\delta^{18}$ O of bulk leaf water ( $\delta^{18}$ O<sub>lw</sub>) as a function of transpiration rate:

197 [5] 
$$\Delta^{18}O_{lw} = (\delta^{18}O_{es} - \delta^{18}O_{sw}) \frac{1 - e^{-\beta}}{\beta} ,$$

where the Péclet number ( $\wp$ ) is a function of transpiration rate (E), the effective pathlength of water molecule movement inside the leaf (L), the molar density of water (C), and the molecular diffusivity of  $H_2^{18}O$  in water (D):

$$201 \quad [6] \qquad \wp = \frac{\mathbf{EL}}{\mathbf{CD}} ,$$

and where E is given by:

203 [7] 
$$E = \frac{\mathbf{g_s} * (\mathbf{e_i} - \mathbf{e_a})}{\mathbf{P}} ,$$

where P is atmospheric pressure.

Thus, in the Péclet-modified CGD model,  $\delta^{18}O_{lw}$  is controlled by the ratio of the advective 205 transpiration flux of unenriched source water, and the back diffusion of <sup>18</sup>O-enriched water 206 from the evaporating site. As transpiration rate increases, the degree of back diffusion of 207 <sup>18</sup>O-enriched water from the evaporating site mixing into the bulk leaf water decreases. 208 Although studies indicate the presence of a Péclet effect in the leaf for many tree species, 209 fewer species exhibit this  $H_2^{18}O$  gradient in the leaf than previously thought (Barbour et al., 210 2021). 211 The  $\delta^{18}$ O signal of sucrose in the leaf is equal to  $\delta^{18}$ O<sub>lw</sub>, plus an additional biochemical 212 fractionation process ( $\varepsilon_{bio}$ ) of 27% that occurs during carbonyl hydration (Sternberg *et al.*, 213 1986). Sucrose is then transported to the cambium where it is assimilated into cellulose. 214

During cellulose synthesis, an estimated fraction of 0.4 ( $p_{ex}$ ) of the exchangeable oxygen in leaf sugars is exchanged with local xylem water at the site of cambial cellulose synthesis (Cernusak *et al.*, 2005). Assuming that xylem water  $\delta^{18}$ O is close to  $\delta^{18}$ O<sub>sw</sub>, i.e. that the proportion ( $p_x$ ) of unenriched source water in local xylem water is 1, the  $p_{ex}p_x$  term is estimated as 0.4. (Roden *et al.*, 2000; Cernusak *et al.*, 2005; Barbour, 2007). Resultantly, the isotopic signature of tree ring cellulose ( $\delta^{18}$ O<sub>trc</sub>) integrates both  $\delta^{18}$ O<sub>sw</sub> and  $\delta^{18}$ O<sub>lw</sub> signals (Barbour & Farquhar, 2000):

222 [8] 
$$\delta^{18}O_{trc} = \Delta^{18}O_{lw}(1 - (p_{ex}p_{x})) + \epsilon_{bio}$$

These models are linked together as displayed in Figure 2.

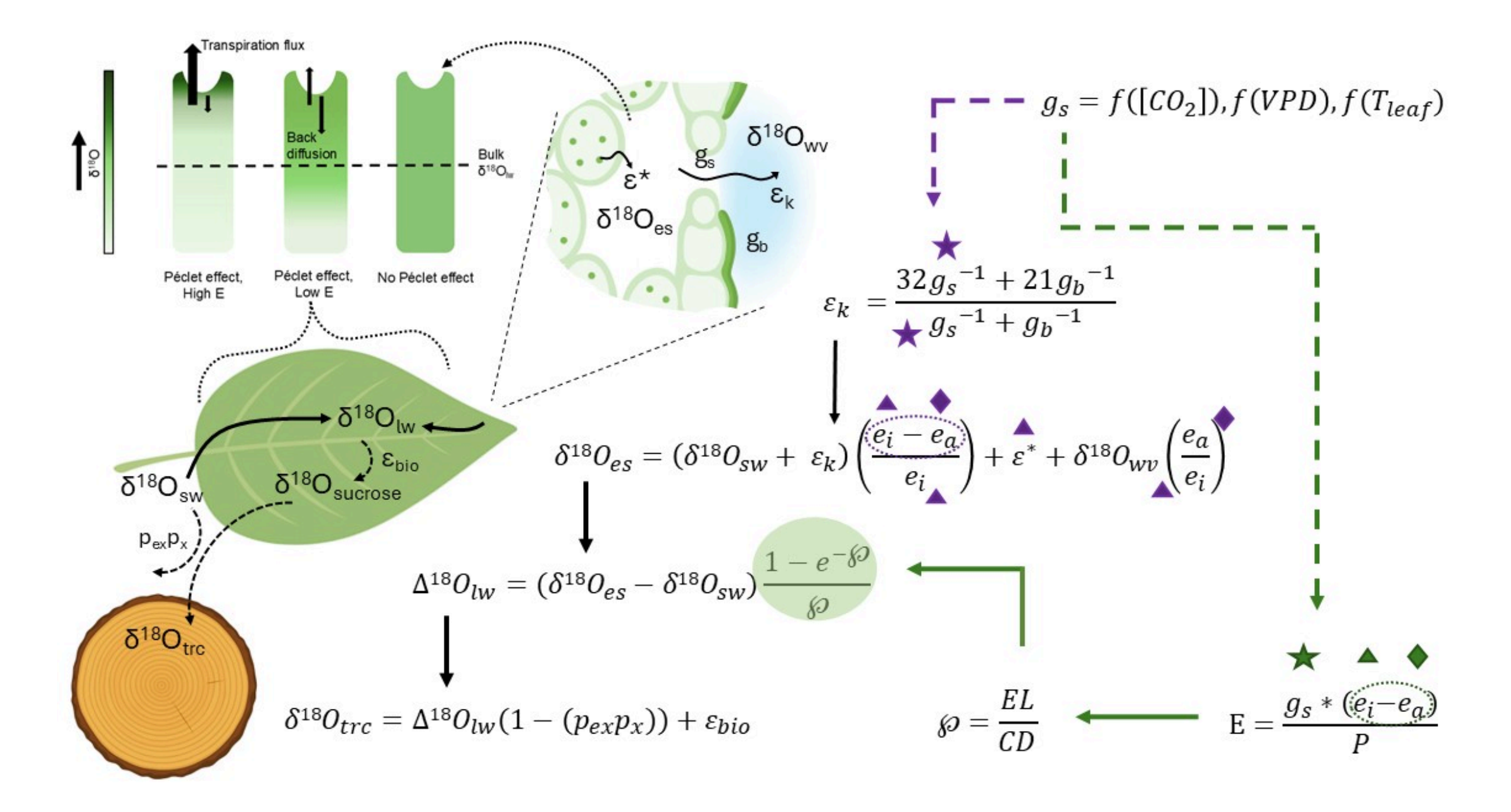


**Figure 2** Models of leaf-level processes and isotopic fractionations that contribute to  $\delta^{18}O_{trc.}$  Depiction of how each isotope model (discussed in the main text) is linked to the oxygen isotope signal of tree ring cellulose. Icons (star, triangle, diamond, stippled circle) indicate the points at which  $g_s$ ,  $T_{leaf}$ ,  $e_a$  and VPD, respectively influence  $\delta^{18}O$ . Dashed arrows indicate the effects of  $g_s$ . Purple arrow and icons indicate points at which the modelled variables affect  $\delta^{18}O$  with or without the Péclet effect. Green arrows and icons indicate points at which the modelled variables affect  $\delta^{18}O$  only when the Péclet effect is present. Diagrams illustrate the locations and processes in which variables in the equations affect  $\delta^{18}O$ . The top left visual demonstrates how transpiration rate (E) and the Péclet effect affect the degree of  $^{18}O$ -enrichment at the evaporating site, and the degree to which this  $^{18}O$ -enriched water pool contributes to bulk leaf water. Abbreviations are listed in Table 1.

Figure 3 shows the theory-predicted isolated effects of stomatal conductance ( $g_s$ ), leaf temperature ( $T_{leaf}$ ), atmospheric vapour pressure ( $e_a$ ) and leaf-to-air vapour pressure deficit (VPD) on  $\delta^{18}O$  at the evaporating site ( $\Delta^{18}O_{es}$ , top row), on bulk leaf water ( $\Delta^{18}O_{lw}$ , middle row), and on tree ring cellulose ( $\delta^{18}O_{trc}$ , bottom row). We illustrate the effects of each variable between the extreme ends of plausible ranges for a typical temperate site, whilst varying  $g_s$  and  $T_{leaf}$  over credible ranges. We compare the effects of each variable both with and without the Péclet effect, and for three different  $g_s$  values, ranging from very low (0.05 mol mr² s-¹), to very high (0.8 mol mr² s-¹), for a temperate climate. The effects shown here do not include physiological plant responses to climate. For example, an increase in VPD would usually cause plants to partially close their stomata (i.e.  $g_s$  decreases) to limit water loss (Buckley, 2019). However, for clarity we here only vary one parameter at a time, holding all other variables constant.

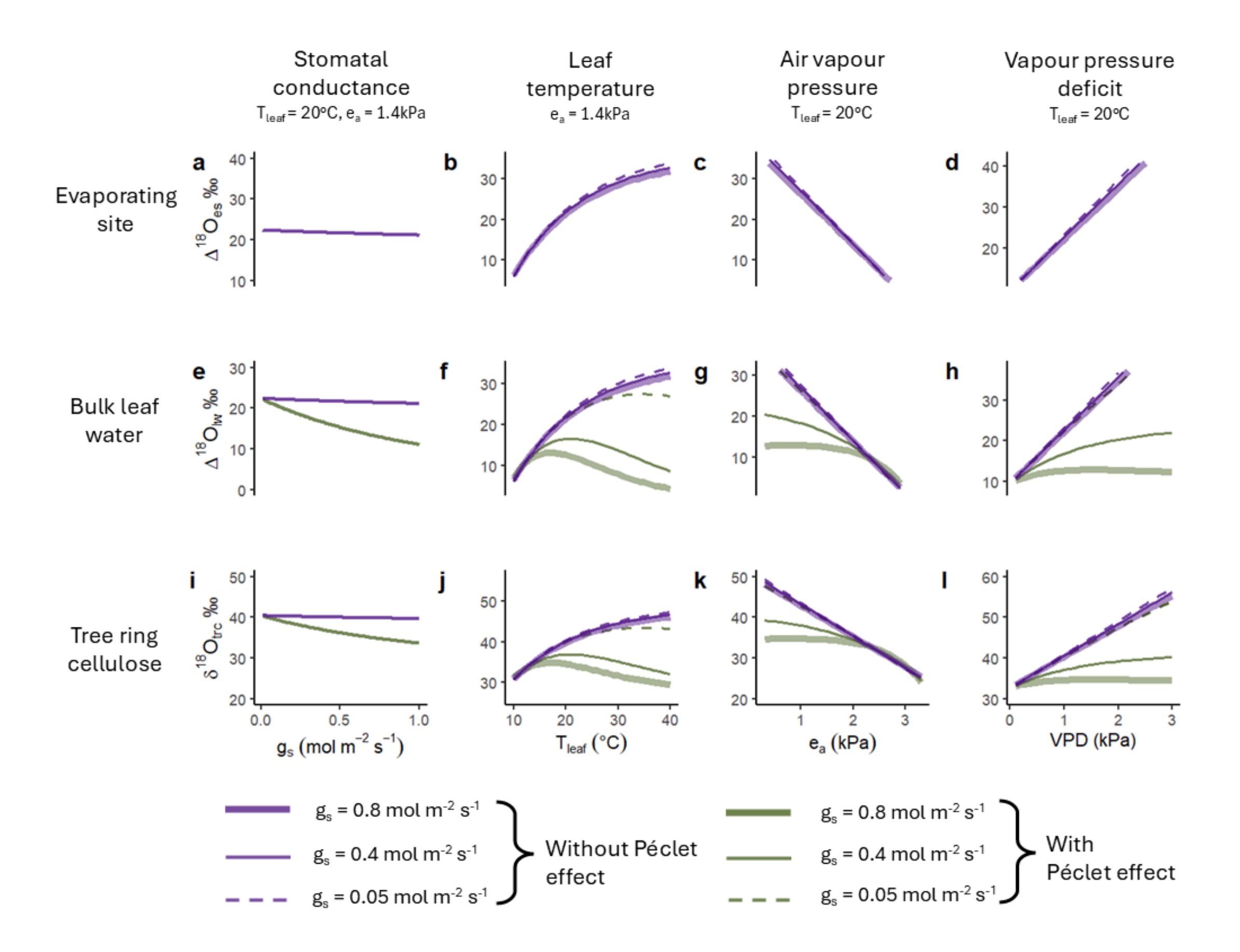


**Figure 3** Model-predicted effects of stomatal conductance ( $g_s$ ), leaf temperature ( $T_{leaf}$ ), atmospheric vapour pressure ( $e_a$ ) and leaf-to-air vapour pressure deficit (VPD) on  $\delta^{18}O$  in the leaf and cambium. The effects of each variable (each column) are simulated for  $\delta^{18}O$  above that of source water in the leaf evaporating site (top row), in bulk leaf water (middle row), and in tree ring cellulose (bottom row). Purple lines illustrate the effects of each variable in the CGD model without a Péclet effect, and green lines illustrate the effects of each variable in the Péclet-modified CGD model. The different line types indicate the modelled effects for different  $g_s$  values. The model assumes that  $\delta^{18}O_{sw}$  and  $\delta^{18}O_{wv}$  are 0%. Therefore, the enrichment above source water ( $\Delta$ ) is equal to the actual leaf water isotope values, i.e.  $\Delta^{18}O_{es} = \delta^{18}O_{es}$ , and  $\Delta^{18}O_{lw} = \delta^{18}O_{lw}$ . VPD is a more useful metric

than  $e_a$  when considering the impact of transpiration on  $\Delta^{18}O_{lw}$ . However, as VPD is a function of both  $T_{leaf}$  and  $e_a$ , we include all three variables for clarity. The Y-axis range for all plots is 30%.

237

238

239

240

241

242

243

244

245

246

248

249

250

251

252

253

254

255

256

257

258

Theory indicates that stomatal conductance ( $g_s$ ) influences  $\delta^{18}O$  only via its effect on transpiration rate (E) caused by the Péclet effect (Fig. 3e-purple vs green line), and has an almost negligible effect on  $\Delta^{18}O_{es}$  (Fig. 3a) via its impact on  $\varepsilon_k$  (Eqn. 3). In the presence of a Péclet effect, increasing g<sub>s</sub> increases E which in turn increases the contribution of unenriched source water from the transpiration stream to bulk leaf water. This weakens the back-diffusion of <sup>18</sup>O-enriched water from the evaporating site into bulk leaf water, thus lowering  $\Delta^{18}O_{lw}$ (Fig.3e). Leaf temperature ( $T_{leaf}$ ) has a positive, non-linear effect on  $\Delta^{18}O_{es}$  (Fig. 3b). This is caused by two effects related to increases in  $T_{leaf}$ , including small changes in  $\epsilon^*$  due to its temperature-dependency, and larger effects arising from increases in ei, which is assumed to be saturated. An increase in  $e_i$  increases the contribution of  $\epsilon_k$  to  $\Delta^{18}O_{es}$ . With the Péclet effect, the relationship between  $T_{leaf}$  and  $\Delta^{18}O_{lw}$  is bell-shaped (Fig. 3f). At lower temperatures,  $\Delta^{18}O_{lw}$  increases, due to increased enrichment at the site of evaporation, while at higher temperatures,  $\Delta^{18}O_{lw}$  decreases. This decrease at higher temperatures is driven by enhanced transpiration rates, resulting in a greater contribution of unenriched source water from the transpiration stream to the leaf. The magnitude of these effects varies depending on g<sub>s</sub>, as discussed at the end of this section. The effect of atmospheric vapour pressure ( $e_a$ ) on  $\Delta^{18}O_{es}$  is negative and linear: as  $e_a$ increases, the contribution of  $\varepsilon_k$  to  $\Delta^{18}O_{es}$  decreases (Fig. 3c). The Péclet effect dampens the effects of  $e_a$  at the evaporating site on  $\Delta^{18}O_{lw}$ , due to increasing E, and thus an increasing contribution of unenriched source water from the transpiration stream to bulk leaf water. This

effect varies depending on  $g_s$ . In contrast, an increase of VPD has a positive linear effect on  $\Delta^{18}O_{es}$  (Fig. 3d). The Péclet effect dampens the effects of VPD at the evaporating site on  $\Delta^{18}O_{lw}$  due to increasing E, and this effect also varies with  $g_s$ .

In the presence of a Péclet effect, there is a significant interactive effect of  $g_s$  with  $T_{leaf}$ ,  $e_a$  and VPD. At larger  $g_s$ , the effect of  $T_{leaf}$ ,  $e_a$  and VPD on  $\Delta^{18}O_{lw}$  weakens. When  $g_s$  is larger, E increases significantly more with increasing  $T_{leaf}$  and VPD (and decreasing  $e_a$ ), resulting in a larger flux of unenriched water into the leaf, which reduces the contribution of increasing

 $\Delta^{18}O_{es}$  into bulk leaf water.

### Methods

267

Sensitivity analysis of tree ring  $\delta^{18}$ O to changes in stomatal conductance and 268 climate 269 The aim of this exercise is to assess the sensitivity of  $\delta^{18}O_{trc}$  trends to changes in  $g_s$  due to 270 global changes since the beginning of the 20th century. We address this aim by modelling an 271 average g<sub>s</sub> response for an idealised mature tree growing in a Northern hemisphere temperate 272 climate, first to changes in  $CO_2$  between 1901 and 2023 (i.e.  $g_s = f(CO_2)$ , c.f. Eqn. SI.3.2), and 273 then to changes in climate (i.e.  $g_s = f(T, VPD)$ , c.f. Eqns. SI.3.3-4) (Figure 4). We do not 274 consider other climatic changes beyond changes in atmospheric vapour pressure (e<sub>a</sub>), 275 temperature and VPD. Therefore, 'climatic changes' and 'Δclimate' refer only to changes in ea, 276 temperature and VPD as occurred since 1901. Then, we simulate the  $\delta^{18}$ O response to the 277 modelled changes in  $g_s$  (i.e.  $\delta^{18}O = f(g_s)$ , c.f. Fig. 2), first at the leaf evaporating site ( $\Delta^{18}O_{es}$ ), 278 then in bulk leaf water ( $\Delta^{18}O_{lw}$ ), and lastly in tree ring cellulose ( $\delta^{18}O_{trc}$ ). Note that we model 279 <sup>18</sup>O-enrichment above source water ( $\Delta^{18}$ O), and that we assume  $\delta^{18}$ O<sub>sw</sub> to be 0%; thus, the real isotopic signal ( $\delta^{18}$ O) is the same value as expressions of the enrichment above source 281 282 water. We examine the sensitivity of  $\Delta^{18}O_{es}$ ,  $\Delta^{18}O_{lw}$  and  $\delta^{18}O_{trc}$  trends to global changes between 283 1901 and 2023, by considering changes in g<sub>s</sub> and changes in climate. To disentangle the 284 isolated effects of CO<sub>2</sub> and climate on g<sub>s</sub> and to disentangle the indirect (i.e. g<sub>s</sub>-moderated) 285 effects on  $\delta^{18}$ O from the direct effects of climate, we developed four models (Table 2). Model 286 1 assesses the  $\delta^{18}$ O sensitivity to changes in  $g_s$  only due to increasing CO<sub>2</sub>. Thus, for model 1 287 we assume that changes in g<sub>s</sub> are dependent only on CO<sub>2</sub> concentration (Eqn. SI.3.2), and 288 changes in  $\delta^{18}$ O are only caused by this  $g_s$ -CO<sub>2</sub> response. All other variables in the  $\delta^{18}$ O 289 equations (Eqns.1-8) are held constant at values given in tables SI.1 and SI.2. Model 2 290 assesses the  $\delta^{18}$ O sensitivity to changes in  $g_s$  only due to climatic changes. Therefore, for 291

model 2, we assume that changes in  $g_s$  are dependent only on temperature and VPD (i.e.  $g_s = f(T, VPD)$ , using Stewart-Jarvis functions (Eqns. SI.3.3-4). As VPD =  $(e_i - e_a)$ , the effects of  $e_a$ on  $g_s$  are inbuilt into the  $g_s$ -VPD function. Thus, for model 2, changes in  $\delta^{18}$ O are only due to this  $g_s$ -climate response, and all other variables in the  $\delta^{18}O$  equations are held constant at values given in tables SI.1 and SI.2. Model 3 assesses the  $\delta^{18}\text{O}$  sensitivity to the total anticipated changes in g<sub>s</sub> due to both CO<sub>2</sub> and climatic changes. Therefore, in model 3, we assume that changes in  $g_s$  are dependent on  $CO_2$ , temperature and VPD (i.e.  $g_s$ =f( $CO_2$ , T, VPD)), and changes in  $\delta^{18}$ O are only due to the total  $g_s$  response. All other variables in the  $\delta^{18}$ O equations are held constant at values given in tables SI.1 and SI.2. Lastly, model 4 assesses the  $\delta^{18}$ O sensitivity to the total anticipated changes in  $g_s$  due to both CO<sub>2</sub> and climatic changes, plus the direct effects of climate on  $\Delta^{18}O_{es}$  in the CGD model (Eqn. 1) and on the rate of transpiration (Eqn. 7). Thus, model 4 assumes that changes in g<sub>s</sub> are dependent on CO<sub>2</sub>, temperature and VPD, and that changes in  $\delta^{18}$ O are due to the total  $g_s$  response plus the changes in temperature,  $e_a$  and VPD directly in the  $\delta^{18}$ O equations. Other variables in the  $\delta^{18}$ O equations are held constant at values given in table SI.2. Thus, model 4 effectively simulates the total expected change in tree ring  $\delta^{18}$ O. We compare the  $\delta^{18}$ O response across six cases (three pairs of cases) for each of the four models (SI.1). For the first and second cases, we compare the sensitivity of  $\delta^{18}$ O for a species with, versus without, a Péclet effect, assuming an average g<sub>s</sub> in 1901 (g<sub>s0</sub>) of 0.3 mol m<sup>-2</sup> s<sup>-1</sup>. For the third and fourth cases, we compare the sensitivity of  $\delta^{18}$ O for a species with a high average  $g_{s0}$  (0.65 mol m<sup>-2</sup> s<sup>-1</sup>), versus a species with a low average  $g_{s0}$  (0.05 mol m<sup>-2</sup> s<sup>-1</sup>). These 'high' and 'low' g<sub>s0</sub> values reflect a representative range observed for gymnosperm and angiosperm trees in temperate climates (Medlyn et al., 2001; Klein & Ramon, 2019; Gardner et al., 2022). For the fifth and sixth cases, we compare the sensitivity of  $\delta^{18}$ O for a tree in a dry (40% RH and 1.41kPa VPD in 1901), versus a wet climate (90% RH and 0.25kPa VPD in 1901),

292

293

294

295

296

297

298

299

300

301

302

303

304

305

306

307

308

309

310

311

312

313

314

315

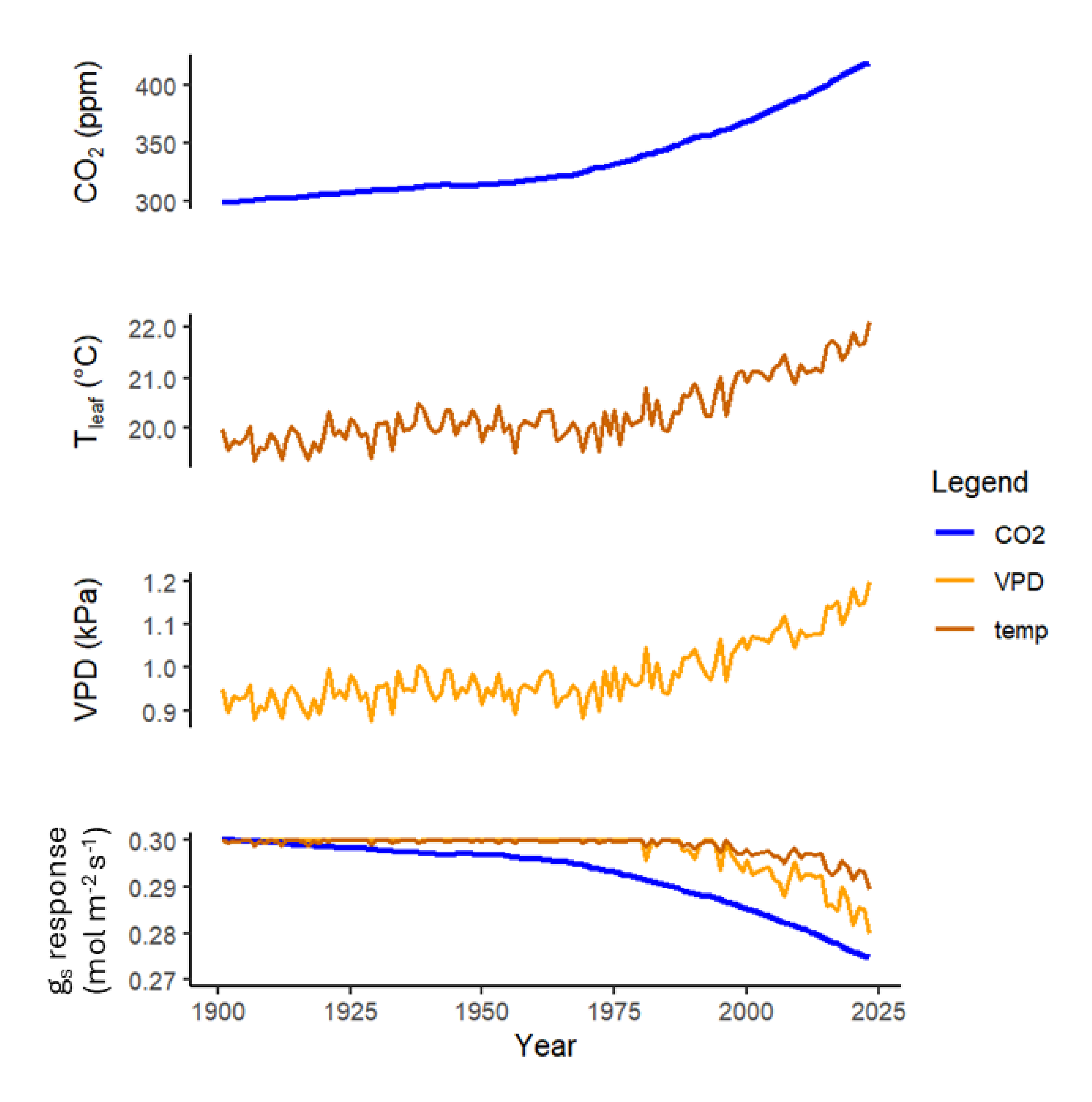


**Figure 4** Historical climate and  $CO_2$  time series, and the modelled  $g_s$  responses used in the simulations. The simulated  $g_s$  changes (bottom panel) are shown for the first and second cases, with a  $g_{s0}$  of 0.3 mol m<sup>-2</sup> s<sup>-1</sup>. The mean global annual atmospheric  $CO_2$  record (top panel) is obtained from a combined ice core dataset extended with data from the Mauna Loa Observatory (Keeling *et al.*, 1976; Etheridge *et al.*, 1996; Ballantyne *et al.*, 2012). The modelled  $g_s$  response to  $CO_2$  (bottom panel-blue) is adapted from Walker *et al.* (2021) (Eqn. Sl.3.2).  $T_{leaf}$  ( $2^{nd}$  panel) is modelled as  $20^{o}$ C plus the annual mean air temperature anomaly for

all land points 23-67°N, from the GISTEMP 250km surface temperature analysis record (GISTEMP Team, 2025). Atmospheric Vapour Pressure ( $e_a$ ) is modelled as 1.4kPa plus the annual mean  $e_a$  anomaly for all land points 23-67°N, from the CRU TS4.08 Vapour Pressure record (Harris *et al.*, 2024). The VPD time series ( $3^{rd}$  panel) is developed from the  $T_{leaf}$  and  $e_a$  models and is illustrated here for the first four cases. The modelled  $g_s$  responses to  $T_{leaf}$  (bottom panel- dark orange) and to VPD (bottom panel- light orange) are Stewart-Jarvis functions (Jarvis, 1976; Stewart, 1988) (Eqns. Sl.3.3-4). The  $g_s$ -climate function used in model 2 (Table 2) combines the VPD and  $T_{leaf}$  response functions (i.e.  $g_s$ =f(VPD, $T_{leaf}$ )). The total  $g_s$  function used in models 3 and 4 (Table 2) combines all three response functions (i.e.  $g_s$ =f(CO<sub>2</sub>, VPD, $T_{leaf}$ )). Climate and CO<sub>2</sub> data was downloaded using KNMI Climate Explorer (https://climexp.knmi.nl/).

**Table 2** Model versions to elucidate the response of  $\delta^{18}O_{trc}$  to changes in  $g_s$  due to climate and  $CO_2$ , and to the direct effects of climate

	Model	Description	Affected variables in isotope model		
		Changes in $\delta^{18}$ O resulting from changes in $g_s$ due to $CO_2$	All cases:		
1	<b>g</b> s	increases	ε <sub>k</sub> via g <sub>s</sub> [CO <sub>2</sub> ]		
			Only cases with a Péclet effect:		
			p via g₅[CO₂]		
	Climate effects	Changes in $\delta^{18}$ O resulting from	All cases:		
2	on g <sub>s</sub>	changes in g <sub>s</sub> due to climatic changes	ε <sub>k</sub> via g <sub>s</sub> [VPD, T]		
			Only cases with a Péclet effect:		

			<i>p</i> via g₅[VPD,T]
	Total g <sub>s</sub> effects	changes in $a_a$ due to $CO_2$	All cases: $\varepsilon_k$ via $g_s[CO_2,VPD,T]$
3		increases&climatic changes	Only cases with a Péclet effect: pvia g <sub>s</sub> [CO <sub>2</sub> VPD,T]
		changes in $a_s$ due to $CO_2$	All cases: $\varepsilon_k$ via $g_s[CO_2,VPD,T]$
4	effects	increases&climatic changes, plus	e <sub>a</sub> . e <sub>i</sub> [T]. ε*[T]
		in CGD model &on rate of transpiration	Only cases with a Péclet effect: $\wp$ via $g_s[CO_2,VPD,T]$ and
			e <sub>i</sub> [T] + e <sub>a</sub>

### Results

342

We examined the contributions of changes in climate and CO<sub>2</sub> between 1901 and 2023 to 343 changes in stable oxygen isotope ratios at the site of evaporation ( $\Delta^{18}O_{es}$ ), in bulk leaf water 344  $(\Delta^{18}O_{lw})$ , and in tree ring cellulose  $(\delta^{18}O_{trc})$ . To disentangle the effects of plant physiology and 345 climate on  $\delta^{18}$ O trends, we simulated the  $\delta^{18}$ O response to changes in  $g_s$  due to  $CO_2$  and 346 climate, and to the direct effects of climate in the CGD model (Eqn. 1) and on the rate of 347 transpiration (Eqn. 7). The climate variables in our model are ea, temperature and VPD, and 348 therefore the effects of climate that we show here are limited to the changes in ea, 349 temperature and VPD since 1901. Below, we first present time trends for the cases with and 350 without the Péclet effect (Fig. 5). We then provide a summary of these effects for three pairs 351 of cases: with versus without Péclet effect (cases 1 vs 2); low versus high g<sub>s</sub> (cases 3 vs 4); 352 and dry versus wet climate (cases 5 vs 6). Figures of the time trends for cases 3-6 are 353 presented in the supplementary material (Figs. SI.4, SI.5). 354 Effects of  $CO_2$  and climate change on tree  $\delta^{18}O$  with and without the Péclet 355 effect 356 According to the stomatal models (c.f. Eqns. Sl.3.2-4) based on compiled average g<sub>s</sub>-CO<sub>2</sub> 357 responses (Walker et al., 2021) and Stewart-Jarvis stomatal conductance functions (Jarvis, 358 1976; Stewart, 1988), increasing CO<sub>2</sub>, VPD and temperature cause g<sub>s</sub> decreases between 359 0.025 and 0.053 mol m<sup>-2</sup> s<sup>-1</sup> (8-18%) over the period 1901 to 2023, depending on the model 360 used (Fig. 5a). These model-predicted decreases in  $g_s$  result in an increase in  $\delta^{18}O_{trc}$  between 361 0.02 and 0.43% (Fig. 5f,g-models 1-3). When the direct effects of climate are also taken into 362 account,  $\delta^{18}O_{trc}$  increases between 0.51 and 0.75% (model 4). 363 Without the Péclet effect, changes in  $g_s$  only influence the kinetic fractionation factor ( $\varepsilon_k$ ), 364 which has a very small effect in the CGD model (Eqn. 1). Resultantly, decreases in g<sub>s</sub> lead to 365 negligible effects on  $\Delta^{18}O_{es}$  (Fig. 5b,d,f- models 1-3). In contrast, when the Péclet effect is 366

present, decreases in g<sub>s</sub> lead to small increases in leaf water <sup>18</sup>O-enrichment (Fig. 5e- models 367 1-3). This effect arises due to a reduced transpiration flux, allowing greater back-diffusion of 368 <sup>18</sup>O-enriched water from the evaporating site into bulk leaf water. 369 The largest effect on  $\delta^{18}$ O is the direct effect of climate, independent of changes in  $g_s$ . Leaf 370 warming and decreases in  $e_a$  elevate VPD, which also enhances the contribution of  $\epsilon_k$  to the 371 isotopic signal at the site of evaporation, leading to an increase of  $\Delta^{18}O_{es}$  by 1.18% (Fig. 5-372 model 4). The direct climate effects most strongly affect  $\Delta^{18}O_{lw}$  and  $\delta^{18}O_{trc}$  in the case without 373 a Péclet effect (Fig. 5d,f-model 4). In contrast, enrichment at the site of evaporation is 374 weakened in  $\Delta^{18}O_{lw}$  and  $\delta^{18}O_{trc}$  in the case with a Péclet effect (Fig. 5c,e,g- model 4). This is 375 because increases in VPD increase the flux of unenriched water from the transpiration stream 376 into the leaf, which weakens the back-diffusion of <sup>18</sup>O-enriched water from the evaporative 377 site. 378

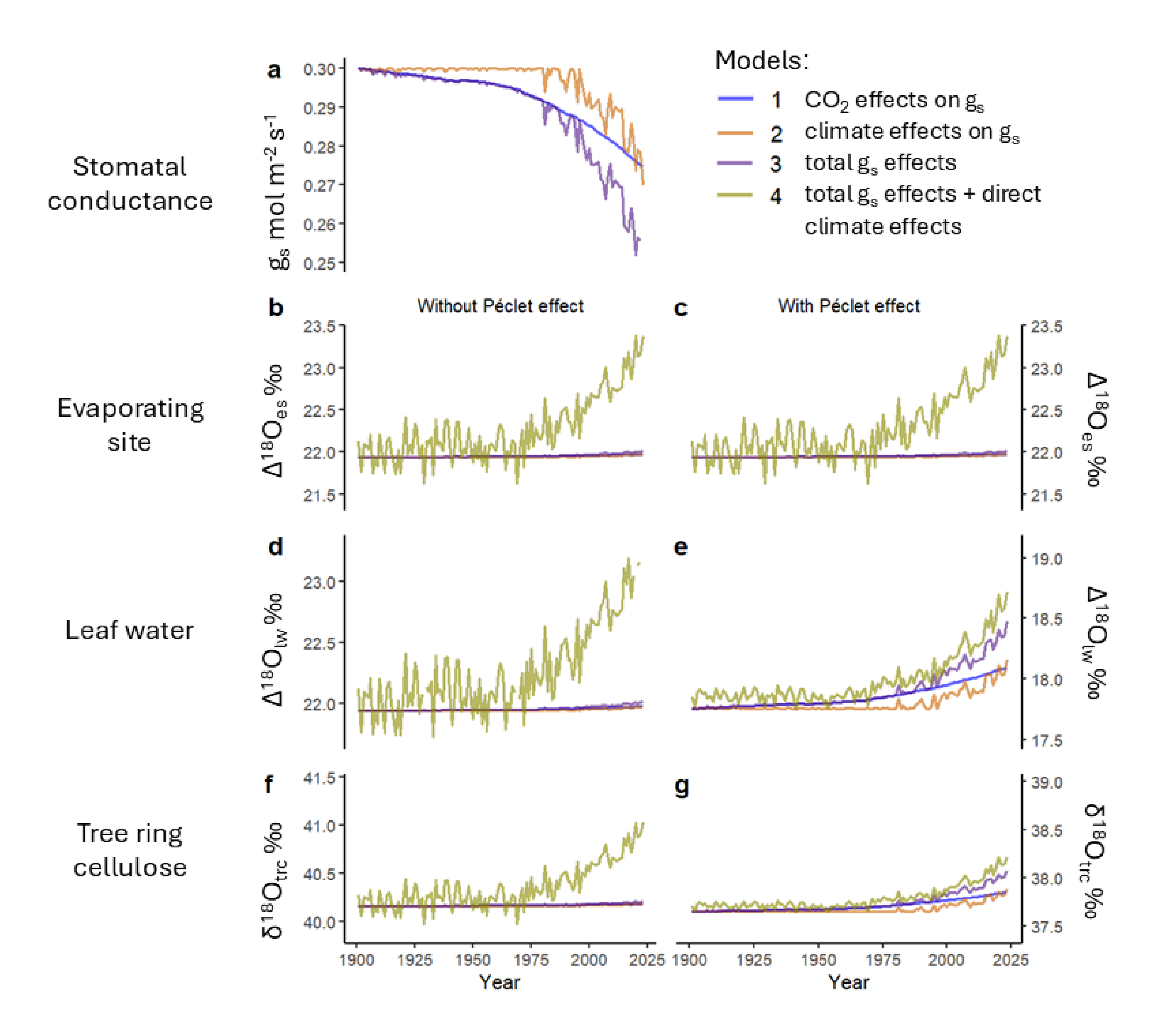


**Figure 5** Predicted  $\delta^{18}$ O changes over the period 1901-2023, with and without the Péclet effect, to changes in  $g_s$  due to  $CO_2$  and climate, and to the direct effects of climate. Subplot a shows the modelled  $g_s$  response to  $CO_2$  (blue), climate (orange), and  $CO_2$  & climate (purple) for both cases. Subplots b-g show the modelled  $\delta^{18}$ O response, without the Péclet effect (b,d,f), and with the Péclet effect (c,e,g), to changes in  $g_s$  and to the direct effects of climate under different levels of sensitivity (models 1-4) in  $\Delta^{18}O_{es}$  (b,c), in  $\Delta^{18}O_{lw}$  (d,e), and in  $\delta^{18}O_{trc}$  (f,g). Without the Péclet effect (left column),  $g_s$  only affects  $\delta^{18}O$  via  $\varepsilon_k$  (Eqn. 2), and VPD,  $e_a$  and temperature exert additional direct influences on  $\delta^{18}O$  via  $\epsilon^{18}O$ -enrichment at the evaporating site in model 4 only (Eqn. 1). With the Péclet effect (right column),  $g_s$  affects  $\delta^{18}O$  via  $\varepsilon_k$  (Eqn. 2) and  $\wp$  (Eqns. 6-7), and – for model 4 only – VPD,  $e_a$  and temperature also influence  $\delta^{18}O$  via  $\epsilon^{18}O$ -enrichment at the evaporating site (Eqn. 1) and  $\wp$  (Eqns. 6-7). The y-axis range for subplots b-c is 2%, and is 1.6% for subplots d-g.

Effects of  $CO_2$  and climate change on tree  $\delta^{18}O$  across cases 394 Stomatal responses to CO<sub>2</sub> and climate change 395 Predicted decreases in g<sub>s</sub> from 1901 to 2023 vary between cases and models (Fig. 6- top 396 panel). In model 1, where we only vary g<sub>s</sub> in response to CO<sub>2</sub> increases from 1901 to 2023, g<sub>s</sub> 397 is reduced by 8%. The absolute changes are smaller (-0.004 mol m<sup>-2</sup> s<sup>-1</sup>) for the low g<sub>s</sub> case, 398 and larger (-0.055 mol m<sup>-2</sup> s<sup>-1</sup>) for the high g<sub>s</sub> case. 399 Increases in temperature and VPD from 1901 to 2023 have an effect on g<sub>s</sub> that is of 400 comparable magnitude as the effect of CO<sub>2</sub> (Fig. 6- top row, models 2 vs 1). VPD is larger in 401 the dry climate case, resulting in a greater decrease in g<sub>s</sub> (-0.033 mol m<sup>-2</sup> s<sup>-1</sup>), compared to the 402 wet climate case (-0.011 mol m<sup>-2</sup> s<sup>-1</sup>). 403 For each case, models 3 and 4 have the same simulated stomatal responses that reflect the 404 combined effects of CO<sub>2</sub> and climatic changes on g<sub>s</sub> (Fig. 6- top panel- models 3,4). From 405 1901 to 2023, the total modelled decrease in g<sub>s</sub> is 12% for the wet climate case, and 18% for 406 all other cases. This results in the largest change in g<sub>s</sub> of -0.114 mol m<sup>-2</sup> s<sup>-1</sup> for the high g<sub>s</sub> case, and the smallest change in g<sub>s</sub> of -0.009 mol m<sup>-2</sup> s<sup>-1</sup> for the low g<sub>s</sub> case. 408 Predicted changes of  $\delta^{18}$ O at the leaf evaporating site, in bulk leaf water and in tree 409 ring cellulose, in response to global change 410 For all cases, changes in  $g_s$  between 1901 and 2023 have a negligible effect on  $\Delta^{18}O_{es}$  (Fig. 6-411 middle panel, models 1-3). In contrast, the direct effects of climate, independent from g<sub>s</sub>, 412 cause relatively large increases in  $\Delta^{18}O_{es}$  between 0.43 and 2.32% (model 4). 413 In bulk leaf water and at the tree ring level, increasing CO<sub>2</sub> and/or changes in climate from 414 1901 to 2023 only cause increases in δ<sup>18</sup>O when the Péclet effect is present (Fig. 6- bottom 415 panel-models 1-3). Furthermore, these effects on  $\delta^{18}$ O are very weak for trees with low 416 average g<sub>s</sub> and in wet climates, again due to the Péclet effect. 417

The increase in  $\Delta^{18}O_{lw}$  is significantly larger for the high  $g_s$  case compared to the low  $g_s$  case, 418 because absolute changes in g<sub>s</sub> due to CO<sub>2</sub> and climate are larger for trees with high g<sub>s</sub> (Fig. 6-419 top&bottom panels, models 1-3). The larger decrease in g<sub>s</sub> for the high g<sub>s</sub> case results in a 420 greater decrease in leaf transpiration rate. Resultantly, there is a greater increase in the 421 back-diffusion of <sup>18</sup>O-enriched water from the evaporating site into the bulk leaf water in the 422 high g<sub>s</sub> case compared to the low g<sub>s</sub> case. 423 VPD is larger in the dry climate case compared to the wet climate case; therefore, the 424 decrease in g<sub>s</sub> between 1901 and 2023 results in a greater decrease in leaf transpiration rate 425 (Eqn. 7). Thus, there is a greater increase in the back-diffusion of 18O-enriched water from the 426 evaporating site into the bulk leaf water for the dry climate case, resulting in a larger increase 427 in  $\Delta^{18}O_{lw}$  compared to the wet climate case (Fig. 6- bottom panel, model 1). 428 The direct effects of climate change on tree  $\delta^{18}$ O 429 Despite the same modelled changes in  $g_s$ , absolute changes in  $\delta^{18}O_{trc}$  for each case differ 430 significantly between models 3 and 4 (Fig. 6- bottom panel, columns 3 vs 4). For the 'without 431 Péclet effect', 'low  $g_s$ ' and 'wet climate' cases, there are large increases in the observed  $\delta^{18}O_{trc}$ 432 signals (model 4), compared to the predicted increases in  $\delta^{18}O_{trc}$  due to changes in  $g_s$  alone 433 (model 3). This is because there are large increases in  $\Delta^{18}O_{es}$  due to the effects of warming 434 and increased VPD between 1901 and 2023, according to the CGD model (Eqn. 1). 435 For the high  $g_s$  and dry climate cases, there are smaller increases in  $\delta^{18}O_{trc}$  for model 4 436 compared to model 3 (Fig. 6- bottom panel, columns 3 vs 4). This is due to the counteracting 437 effects of decreasing g<sub>s</sub> and increasing VPD in Eqn. 7 for model 4, which weakens the 438 decrease in leaf transpiration rate compared to model 3. Resultantly, for model 4, there is a 439 smaller increase to the back-diffusion of <sup>18</sup>O-enriched water from the evaporating site into 440 bulk leaf water. 441

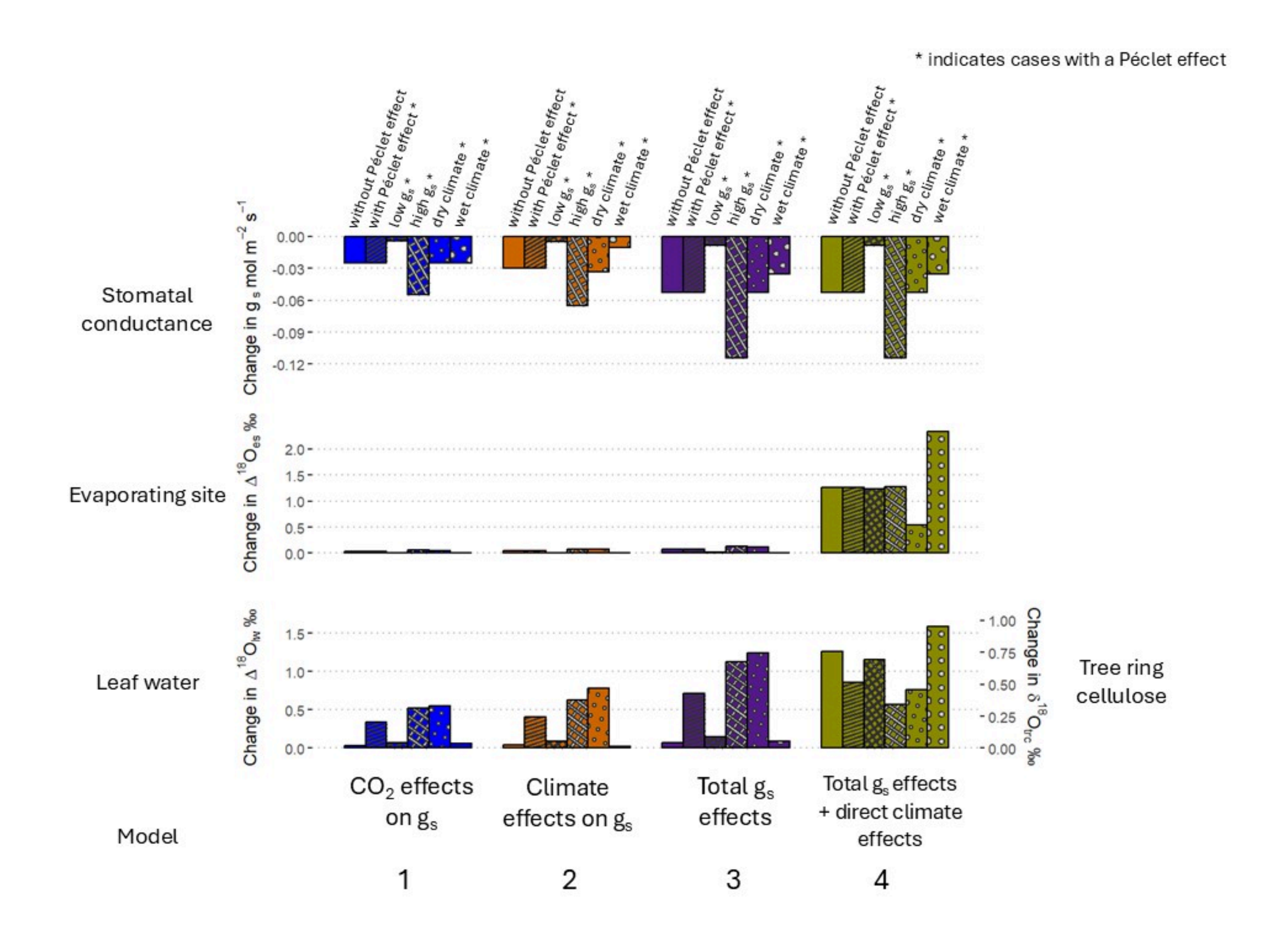


**Figure 6** Modelled net changes between 1901 and 2023 in stomatal conductance and  $\delta^{18}$ O for each of the six cases, across the four models. Changes are shown for six cases, indicated at the top of the panel (without Péclet effect- blank, with Péclet effect- stripe, low  $g_s$ -thin crosshatch, high  $g_s$ - thick crosshatch, dry climate- small dot, wet climate- large dot). For all panels, each bar illustrates the predicted *net change* between 1901 and 2023 in  $g_s$  (top),  $\Delta^{18}O_{es}$  (middle),  $\Delta^{18}O_{lw}$  (bottom- left) and  $\delta^{18}O_{trc}$  (bottom- right) for each case due to:  $CO_2$  effects on  $g_s$  (model 1- blue), climate effects on  $g_s$  (model 2- orange), total - i.e.  $CO_2$  & climate - effects on  $g_s$  (model 3- purple), and total effects on  $g_s$  plus the direct effects of climate in the CGD model (Eqn. 1) and on the rate of transpiration (Eqn. 7) (model 4- yellow).

Across cases, the sensitivity of  $\delta^{18}O_{trc}$  to a given decrease in  $g_s$  varies (Table 3). For the case 445 without a Péclet effect,  $\delta^{18}O_{trc}$  increases by 0.86% per 1 mol m<sup>-2</sup> s<sup>-1</sup> decrease of g<sub>s</sub>, i.e. 446  $\Delta\delta^{18}O_{trc}/\Delta g_{s-total} = -0.86\%$  (mol m<sup>-2</sup> s<sup>-1</sup>)<sup>-1</sup>. For the case with a Péclet effect,  $\Delta\delta^{18}O_{trc}/\Delta g_{s-total} =$ 447 -8.14% (mol m<sup>-2</sup> s<sup>-1</sup>)<sup>-1</sup>. With all other conditions being the same for these two cases, the 448 sensitivity of  $\delta^{18}O_{trc}$  to a given change in  $g_s$  is 9.5x greater when there is a Péclet effect in the 449 leaf (Table 3- columns 1 vs 2). The sensitivity of  $\delta^{18}O_{trc}$  to a given change in  $g_s$  is 1.8x greater 450 for the low  $g_s$  case ( $g_{s0}$  = 0.05 mol m<sup>-2</sup> s<sup>-1</sup>) compared to the high  $g_s$  case ( $g_{s0}$  = 0.65 mol m<sup>-2</sup> 451 s<sup>-1</sup>) (Table 3- columns 3 vs 4). Nonetheless, according to our model, changes in g<sub>s</sub> due to CO<sub>2</sub> 452 453 and climate are larger for the high  $g_s$  case, such that changes in  $\delta^{18}O_{trc}$  are also greater compared to the low g<sub>s</sub> case (Fig.3 bottom panel- models 1-3). For the same change in g<sub>s</sub>, the 454 sensitivity of  $\delta^{18}O_{trc}$  is 9.3x greater for the dry climate case (40% RH in 1901) compared to the 455 wet climate case (90% RH in 1901) (Table 3- columns 5 vs 6). 456

458

Table 3 Sensitivity of  $\delta^{18}O_{trc}$  to modelled changes in  $g_s$  for each case

# Change in $\delta^{18}O_{trc}$ per change in $g_s$ ( $\Delta\delta^{18}O_{trc}/\Delta g_s$ )

% (mol m<sup>-2</sup> s<sup>-1</sup>)<sup>-1</sup>

	Standard	Standard	Low g <sub>s</sub>	High g <sub>s</sub>	Wet climate	Dry climate
	without Péclet effect		with	n Péclet effe	ect	
Sensitivity to $CO_2$ effects on $g_s$ $\Delta \delta^{18}O_{trc}/\Delta g_{s\text{-}CO2}$	-0.85	-8.01	-10.38	-5.72	-1.53	-13.15
Sensitivity to climate effects on $g_s$ $\Delta \delta^{18} O_{trc} / \Delta g_{s\text{-climate}}$	-0.85	-8.04	-10.38	-5.75	-1.52	-14.07
Sensitivity to total $g_s$ effects $\Delta \delta^{18} O_{trc}/\Delta g_{s\text{-total}}$	-0.86	-8.14	-10.38	-5.89	-1.53	-14.28

# Discussion

461

462

Results summary

463	We find that changes in $g_s$ due to $CO_2$ and climate between 1901 and 2023 only significantly
464	contribute to $\delta^{18} O_{\text{trc}}$ trends for species with a pronounced Péclet effect. Indeed, we find that
465	$\delta^{18}O_{trc}$ is 9.5x more sensitive to changes in $g_s$ when the Péclet effect is present. This is
466	because changes in $g_{\rm s}$ only have a significant effect on leaf water $^{18}\text{O-enrichment}$ by causing
467	changes in transpiration flux (Eqn. 7) which moderates the degree of back-diffusion of
468	$^{18}\text{O-enriched}$ water from the evaporating site into bulk leaf water (Eqn. 6). Although $\delta^{18}\text{O}_{trc}$ is
469	1.8x more sensitive to a given change in $g_{s}$ for species with a low average $g_{s}$ , changes in $g_{s}$
470	are easier to detect in $\delta^{18} O_{trc}$ trends for species with a high average $g_s$ because $CO_2$ and
471	climate cause larger changes to $g_{\text{s}}$ . These species with larger $g_{\text{s}}$ changes exhibit larger
472	changes in $\delta^{18}\text{O}_{\text{trc}}$ because of the greater reduction in transpiration flux, resulting in greater
473	increases in bulk leaf water $\delta^{18}\text{O}.$ This is of course only true under the assumption that $g_s$
474	responses are scaled proportionately to average $g_s.$ Lastly, we find that $\delta^{18}O_{trc}$ is 9.3x more
475	sensitive to the same changes in $g_s$ for a tree situated in a dry climate versus a wet climate.
476	This is because VPD is greater in drier climates, and thus, a given change in $g_{\rm s}$ causes a
477	greater change in transpiration rate in a dry compared to a wet (i.e. low VPD) climate (Eqn. 7).
478	Resultantly, in drier climates, a given change in $g_{\rm s}$ corresponds to a greater change in the
479	degree of back-diffusion of $^{18}\mathrm{O}\text{-enriched}$ water from the evaporating site into the bulk leaf
480	water (Eqn. 6).
481	Key issues for using tree ring $\delta^{18}\text{O}$ to infer long-term stomatal conductance
482	trends
483	Our results show that there are three main issues associated with detecting climate and
484	$\text{CO}_2\text{-induced}$ changes in $g_s$ from $\delta^{18}\text{O}_{trc}$ trends. These issues are in addition to the errors
485	associated with estimates of historical source water $\delta^{18}$ O trends, as addressed by Lin <i>et al</i> .

(2022). First, changes in  $\delta^{18}O_{trc}$  caused by changes in  $g_s$  are small compared to the 0.3‰ measurement precision (Boettger *et al.*, 2007). The second and most significant issue is that changes in  $\delta^{18}O_{trc}$  caused by changes in  $g_s$  are small in comparison to changes in  $\delta^{18}O_{trc}$  caused by the direct effects of increasing VPD and temperature in the CGD model (Eqn. 1) and on the Péclet effect (Eqn. 6). A third related issue is the high interannual variability of long-term VPD and temperature increases, which adds further complexity to disentangling a  $g_s$  signal from  $\delta^{18}O_{trc}$  trends. Thus, without independent, reliable estimates of VPD and temperature, detecting long-term changes in  $g_s$  from  $\delta^{18}O_{trc}$  trends is not possible.

### Implications of our findings

486

487

488

489

490

491

492

493

494

495

496

497

498

499

500

501

502

503

504

505

506

507

508

509

510

511

Our results have significant implications for the conclusions in Mathias & Thomas (2021) and Guerrieri et al. (2019). The studies use tree ring  $\delta^{13}$ C and  $\delta^{18}$ O<sub>trc</sub> trends to conclude that increases in iWUE under anthropogenic climate change and rising CO<sub>2</sub> levels are primarily due to increases in assimilation rate (A), whereas g<sub>s</sub> remains effectively unchanged or only decreases in water-limited sites. However, the results of our simulation cases suggest that changes in  $g_s$  due to  $CO_2$  and climate are only detectable in  $\delta^{18}O_{trc}$  trends for trees growing in dry climates, and not in wet climates. Thus, it is well possible that g<sub>s</sub> has decreased in more sites than recognised in these studies but was simply not detectable in the observed δ18Otrc trends. This reasoning is previously demonstrated in sensitivity analyses whereby plant  $\delta^{18}$ O is modelled as a function of  $g_s$  and RH, demonstrating that  $\delta^{18}O$  is significantly more responsive to the same change in  $g_s$  under low RH – i.e. dry, moisture-limited conditions – versus under high RH – i.e. wet conditions (Roden & Siegwolf, 2012; Barbour et al., 2000). Experimental evidence indeed demonstrates that changes in  $g_s$  are more detectable in plant  $\delta^{18}O$  in drier conditions. For example,  $\delta^{18}O$  of cellulose in cotton leaves was more sensitive to decreases in g<sub>s</sub> under 43% RH versus under 76% RH (Barbour&Farquhar, 2000). However, it is important to note that the conclusions that  $g_s$  did not change for most sites in Mathias & Thomas (2021) and Guerrieri et al. (2019) may still be correct. Indeed, it is reasonable to expect based on

physiological principles that trees would avoid reducing g<sub>s</sub> when water is not a limiting factor, in order to maintain their supply of CO<sub>2</sub> into the leaf for photosynthetic assimilation. However, our results demonstrate that  $\delta^{18}O_{trc}$  trends cannot be used to detect the small decreases in  $g_s$ as expected from increases in CO<sub>2</sub> since pre-industrial levels. Given these current methodological limitations, we strongly caution against such applications of  $\delta^{18}O_{trc}$  trends to infer long-term changes in  $g_s$  as a result of changes in  $CO_2$ . Our study further exemplifies that the effects of increasing VPD and temperature at the leaf evaporating site have a significantly greater impact on  $\delta^{18}O_{trc}$  and  $\Delta^{18}O_{lw}$  trends than do the effects of changes in g<sub>s</sub> due to CO<sub>2</sub> and climate. Although it would be plausible to infer decreases in  $g_s$  from increases in  $\delta^{18}O_{trc}$  caused primarily by long-term trends of increasing VPD, this is not a direct detection of changes in  $g_s$ . Indeed, it is also plausible that  $g_s$  may not change under long-term VPD increases. For example, g<sub>s</sub> may acclimatise to long-term exposures of rising VPD (Marchin et al., 2016). Additionally, more anisohydric tree species, that can withstand highly negative water potentials and are thus less vulnerable to xylem embolism, may opt to keep their stomata open under increasing VPD and diminishing plant water status to maintain carbon gain and growth (Tardieu and Simonneau, 1998; McDowell et al., 2008). Thus, a clear VPD-driven  $\delta^{18}O_{trc}$  trend is not a conclusive indicator of a long-term  $g_s$ trend because VPD can affect  $\delta^{18}O_{trc}$  without affecting  $g_s$  (c.f. Fig. 6- models 3 vs 4). Disentangling the effects of  $g_s$  changes on  $\delta^{18}O_{trc}$  trends is further complicated because the high interannual variability of VPD and temperature causes high interannual variability of  $\delta^{18}O_{trc}$  signals (see Fig.5). Therefore, long-term increases and year-to-year variation in VPD and atmospheric temperatures present significant challenges for attempts to correctly attribute the changes in  $\delta^{18}O_{trc}$  that are due to changes in  $g_s$ .

535

536

512

513

514

515

516

517

518

519

520

521

522

523

524

525

526

527

528

529

530

531

532

533

Our analysis shows that the existing methods to use  $\delta^{18}O_{trc}$  trends to predict how  $g_s$  is changing with rising CO<sub>2</sub> levels and climatic changes are too uncertain to currently be used (Lin et al., 2022; Roden et al., 2022). This finding is relevant for interpreting tree ring  $\delta^{18}$ O trends because our simulations compare well with observed trends in published  $\delta^{18}O_{trc}$ records (SI.6), indicating that the parameters of the model and simulations are within the realm of observations from field studies. Despite the relatively large variation in  $\delta^{18}O_{trc}$ changes between studies, potentially caused in part by variation in  $\delta^{18}O_{sw}$  changes, the 50-year change in  $\delta^{18}O_{trc}$  predicted by our model is close to the mean  $\delta^{18}O_{trc}$  change for 172 global tree ring chronologies from 136 sites and 15 tree species (Guerrieri et al., 2019; Mathias & Thomas, 2021; Treydte et al., 2023) (Fig. Sl.6). Thus, the issues associated with using  $\delta^{18}O_{trc}$ trends to infer long-term changes in g<sub>s</sub> as revealed by our study reflect real issues that can lead to erroneous interpretations of  $\delta^{18}O_{trc}$  records. However, there are some limitations to the modelling assumptions that we use for this analysis although they are not critical to our overall conclusions. Firstly, the focus of this analysis is for temperate climates, which may limit the applicability of our findings. Therefore, we checked whether our findings also hold for warmer, tropical climates (SI.7). We find similar trends and magnitudes of change in  $\delta^{18}O_{trc}$  across cases and models for the tropical and temperate simulations (Figs. SI.7i and SI.7ii), indicating that it is also not possible to unambiguously disentangle long-term  $g_s$  trends from tropical  $\delta^{18}O_{trc}$  records. Secondly, Stewart-Jarvis functions were used to an approximate g<sub>s</sub> responses to increasing temperatures and VPD between 1901 and 2023. However, g<sub>s</sub> is sensitive to other variables such as light and soil water potential which were part of the original Stewart-Jarvis model (Jarvis, 1976; Stewart, 1988). We did not use these functions in our simulations, first because we do not expect light intensity to have changed significantly over the last 100 years, and second because simulating soil water trends requires site-specific assumptions of the soil

537

538

539

540

541

542

543

544

545

546

547

548

549

550

551

552

553

554

555

556

557

558

559

560

properties and the implementation of complex hydraulic models which are beyond the capacity and purpose of this study. Finally, Stewart-Jarvis functions are constructed based on diurnal responses of  $g_s$  to environmental variables, while we use these functions to model long term  $g_s$  responses. , Thus, if  $g_s$  does acclimatise to long-term increases in temperature and VPD (Marchin et~al., 2016), then  $g_s$  changes are expected to be smaller than modelled, reinforcing our core message that  $g_s$  responses to anthropogenic global changes are too small to significantly contribute to observed  $\delta^{18}O_{trc}$  trends. In contrast, the direct effects of climate have a far greater contribution to changes in  $\delta^{18}O_{trc}$ . Therefore, any small  $\delta^{18}O_{trc}$  trend due to long-term  $g_s$  changes is obscured by larger  $\delta^{18}O_{trc}$  trends driven by the direct effects of increasing VPD and temperature in Eqns. 1 and 7, and also by noisiness in the  $\delta^{18}O_{trc}$  signal due to interannual climatic variability.

The modelled  $g_s$  response to  $CO_2$  is derived from the C3 plant  $CO_2$ - $g_s$  response curve in Walker et~al. (2021), which integrates observed  $CO_2$ - $g_s$  relationships from a wide range of studies, and which sits within the range of stomatal sensitivities to  $CO_2$  measured in laboratory settings for 57 angiosperm and gymnosperm tree species (Klein & Ramon, 2019). Thus, our model should

Further uncertainties, recommendations for future studies, and methodological

reflect a general g<sub>s</sub>-CO<sub>2</sub> response in trees, although this will vary between species and with

other tree physiological parameters (e.g. tree size, age and health). For example, some studies

find weaker, or even negligible, g<sub>s</sub> responses to changes of CO<sub>2</sub> in mature trees of temperate

regions (Keel et al., 2007; Bader et al., 2013; Streit et al., 2014; Klein et al., 2016).

## improvements

There are additional considerations that we did not address in this study, but which constitute further uncertainties for the use of  $\delta^{18}O_{trc}$  trends as a proxy for long-term  $g_s$  changes. The effective pathlength (L) in the Péclet term varies between species (Kahmen *et al.*, 2009).

Moreover, there is evidence that L can vary within a species with changes in transpiration rate and needle age (Song et al., 2013; Roden et al., 2015). If this is the case, the response of  $\Delta^{18}O_{lw}$  and  $\delta^{18}O_{trc}$  to changes in  $g_s$  is further dampened, as demonstrated in Lin *et al.* (2022). Additionally, there is evidence that several environmental and physiological factors may drive variation in the proportion of oxygen that exchanges with source water during cambial cellulose synthesis ( $p_{ex}p_x$ ). This degree of exchange has been shown to be dependent on the type of species (Wang et al., 1998; Gessler et al., 2013), the time and transport distance between sucrose synthesis in the leaf and its incorporation into cambial cellulose (Farquhar et al., 1998; Barbour & Farquhar, 2000; Barnard et al., 2007; Song et al., 2014), the site aridity (Cheesman & Cernusak 2016), and  $CO_2$  concentration (Morgner *et al.*, 2024). The  $\delta^{18}O_{trc}$ model (Eqn. 8) assumes that a constant fraction (0.4) of the oxygen in cellulose is exchanged with source water based on experimental evidence (Roden & Ehleringer, 1999; Cernusak et al., 2005). Resultantly, unaccounted variability in  $p_{ex}p_x$  may result in erroneous interpretations of  $\Delta^{18}O_{lw}$  (and thus,  $g_s$ ) from  $\delta^{18}O_{trc}$  records. Future research efforts should investigate the impact of these remaining uncertainties on interpretations of  $g_s$  from long-term in-situ  $\delta^{18}O_{trc}$  trends, e.g. by repeating a similar sensitivity analysis that simulates  $\delta^{18}O_{trc}$  trends with L and  $p_{ex}p_x$  varying with climatic changes and transpiration rate. Experimental studies would be particularly useful to assess whether the proportion of oxygen exchanged with source water during cambial cellulose synthesis (i.e.  $p_{ex}p_{x}$ ) indeed changes with long-term exposures to  $CO_{2}$  and climatic changes. Additionally, the research field would benefit from a large-scale quantification of Péclet effects across tree species, sites and climatic conditions, and from identifying how well the Péclet model predicts leaf  $\delta^{18}$ O gradients averaged over growing seasons. Lastly, we suggest experimentally validating the results of this study, for example by comparing  $g_s$  and  $\Delta^{18}O_{lw}$  measurements between ambient and elevated CO<sub>2</sub> conditions at Free Air CO<sub>2</sub> Enrichment (FACE) facilities (e.g. Battipaglia et al., 2013). Such experiments could provide insight into whether

587

588

589

590

591

592

593

594

595

596

597

598

599

600

601

602

603

604

605

606

607

608

609

610

611

CO<sub>2</sub>-induced changes in  $g_s$  are indeed indetectable in  $\Delta^{18}O_{lw}$  (and, thus,  $\delta^{18}O_{trc}$ ). These, and

further research recommendations are summarised in Table 4.

615

**Table 4:** Unresolved issues for  $\delta^{18}O_{trc}$ -derived estimates of  $g_s$  changes and suggested future experiments

Explanation	Recommendations for future research
-No long-term records of	-Explore whether position-specific δ <sup>18</sup> O <sub>trc</sub>
changes in $\delta^{18}O_{sw}$ used by trees	approaches (e.g. Sternberg <i>et al.</i> , 2003, 2007;
	Waterhouse <i>et al.</i> , 2013) allow to calculate
	δ <sup>18</sup> O <sub>sw</sub> incorporated into annual tree ring
	cellulose
	-Collect and analyse long-term rainfall δ <sup>18</sup> O
	(δ <sup>18</sup> O <sub>p</sub> ) at more sites (c.f. GNIP*), to
	understand how $\delta^{18}O_p$ varies with climate,
	which may allow improving historical
	reconstructions
-Unknown degree of Péclet	-Quantification of Péclet effects across more
effects for many tree species	tree species
-Unknown effects of L variability	- <i>In-situ</i> observations of how leaf δ <sup>18</sup> O varies
on bulk leaf δ <sup>18</sup> O	temporally (diurnally, seasonally) and between
	species
-Unclear how p <sub>ex</sub> p <sub>x</sub> varies across	- <i>In-situ</i> isotope labelling and tracing studies to
and within species under	quantify degree of oxygen exchanged with
environmental changes	source water over the growing season and in
	response to climatic changes
	changes in $\delta^{18}O_{sw}$ used by trees -Unknown degree of Péclet effects for many tree species -Unknown effects of L variability on bulk leaf $\delta^{18}O$ -Unclear how $p_{ex}p_x$ varies across and within species under

Empirical evidence of	-Lack of empirical evidence of	-Utilisation of CO <sub>2</sub> fertilisation (FACE)
how CO <sub>2</sub> and	CO <sub>2</sub> and climate-induced	experiments to analyse g <sub>s</sub> and Δ <sup>18</sup> O <sub>lw</sub> trends
climate-induced g <sub>s</sub>	stomatal changes having driven	between ambient and elevated CO <sub>2</sub> levels
changes contribute to	changes in $\delta^{18}O_{lw}$ and $\delta^{18}O_{trc}$ in	under <i>in-situ</i> conditions
δ <sup>18</sup> O <sub>trc</sub> trends	field observations	

\*GNIP: Global Network of Isotopes in Precipitation (www.iaea.org/services/networks/gnip)

617

618

619

620

621

622

624

625

626

627

628

629

630

631

632

633

634

Despite the significant limitations for current methods attempting to derive changes in g<sub>s</sub> from  $\delta^{18}O_{trc}$  trends, steps may be taken to improve the detection of changes in  $g_s$  using this approach. Firstly, our results show that  $\delta^{18}O_{trc}$  is most sensitive to a given change in  $g_s$  for species with a Péclet effect and a high average g<sub>s</sub>, and for trees situated in dry climates. Thus, assuming the issues regarding the effects of climatic changes on  $\delta^{18}O_{trc}$  trends can also be addressed, preliminary considerations can be made to select tree species and sites where  $\delta^{18}O_{trc}$  would be most sensitive to potential  $g_s$  changes. For example, leaf hydraulic design (Zweiniecki et al., 2007) may moderate the presence of a Péclet effect in the leaf (Holloway-Philipps et al., 2016; Barbour et al., 2021, 2024). Of the species tested in Barbour et al. (2021) and (2024), the hydraulic designs of gymnosperms are generally not associated with whole-leaf Péclet effects, whereas the hydraulic designs of angiosperms are generally conducive to whole-leaf Péclet effects. Although these implications need to be tested in-situ and for more species, these findings alongside the results of our study suggest that long-term  $g_s$  trends may be better detected in  $\delta^{18}O_{trc}$  chronologies of angiosperms with hydraulic designs that facilitate whole-leaf Péclet effects. Site-level considerations to optimise the detection of long-term changes in  $g_s$  from  $\delta^{18}O_{trc}$  trends should include selecting drier regions with minimal year-to-year climatic variability, and avoiding sites predisposed to environmental

stressors such as low nutrient availability, long-term drought and pollution (see Siegwolf *et al.,* 2023 for a comprehensive overview of environmental considerations).

Another potentially promising avenue to improve the detection of  $g_s$  changes from  $\delta^{18}O_{trc}$ trends is position-specific  $\delta^{18}$ O analysis (i.e. analysis of  $\delta^{18}$ O at each oxygen position in the cellulose repeating unit). This method could allow disentangling  $\delta^{18}O_{sw}$  and  $\delta^{18}O_{lw}$  signals from tree ring cellulose, and would thus be able to overcome the interfering influence of variation in source water  $\delta^{18}$ O over time. There is evidence that specific positions of the cellulose monomeric unit undergo complete exchange with xylem water during heterotrophic cellulose synthesis in wheat, whereas other positions do not exchange with xylem water (Waterhouse et al., 2013; Sternberg et al., 2003). Thus, positions where there is complete exchange reflect a pure  $\delta^{18}O_{sw}$  signal, and positions where there is no exchange retain  $\delta^{18}O$  of the material from which the cellulose was formed. It remains yet to be tested whether exchange with xylem water also occurs at specific positions of the monomeric unit during cambial cellulose synthesis. If similar exchange processes also occur for trees, then some positions of the tree ring cellulose monomeric unit could reflect a true δ<sup>18</sup>O<sub>sw</sub> signal, and other positions could reflect a true  $\delta^{18}O_{lw}$  signal. A position-specific approach suitable for tree ring studies could improve the ability to detect longer trends of changes in g<sub>s</sub> in two important ways. Firstly,  $\Delta^{18}O_{lw}$  is nearly two times more sensitive than  $\delta^{18}O_{trc}$  to changes in  $g_s$  (Fig. 6). Secondly, this approach would provide actual  $\delta^{18}O_{sw}$  values used by the plant. Therefore, this would avoid the use of untested and unreliable isotope-climate models to reconstruct historical trends in  $\delta^{18}O_{sw}$ , which are required to calculate  $\Delta^{18}O_{lw}$  and  $g_s$ .

## Conclusions

635

636

637

638

639

640

641

642

643

644

645

646

647

648

649

650

651

652

653

654

655

656

657

658

659

Using current tree ring oxygen isotope models, we find that using long-term  $\delta^{18}O_{trc}$  trends is not a suitable method to infer  $g_s$  responses to  $CO_2$  and climate change, because in many cases the sensitivity of  $\delta^{18}O_{trc}$  trends to changes in  $g_s$  is too weak to be detectable. Without a

Péclet effect, δ<sup>18</sup>O<sub>trc</sub> is unresponsive to changes in g<sub>s</sub>, and even when a Péclet effect is 660 included,  $\delta^{18}O_{trc}$  is significantly less sensitive to changes in  $g_s$  in wetter climates, compared to 661 the same  $g_s$  change in a dry climate. Thus, even when there is no significant trend in  $\delta^{18}O_{trc}$ ,  $g_s$ 662 may have changed but simply did not elicit a large enough change in  $\delta^{18}O_{trc}$  to be detected. 663 Yet, even in contexts where  $\delta^{18}O_{trc}$  is sufficiently responsive to changes in  $g_s$ , the enrichment 664 effects of VPD and temperature at the leaf evaporating site have a far greater effect on  $\delta^{18}O_{trc}$ , 665 such that any trends in  $\delta^{18}O_{trc}$  cannot be unambiguously attributed to  $CO_2$  or climate-driven 666 changes in  $g_s$ . Thus, we do not recommend the use of  $\delta^{18}O_{trc}$  trends as a suitable indicator for 667 668 long-term responses of g<sub>s</sub> to CO<sub>2</sub> and climatic changes.

## **Declarations**

- 670 **Acknowledgements** This work was supported by funding from The Leverhulme Trust
- 671 (Research Project Grant Number: RPG-2023-081)
- 672 **Availability of data and material** Upon acceptance, the code and data will be uploaded to an
- 673 openly available data repository.
- 674 Author information
- Authors and affiliations School of Geography, University of Leeds, Garstang Building,
- 676 Woodhouse, Leeds, England, LS2 3AA
- 677 Imogen Carter, Roel Brienen, Manuel Gloor
- 678 **Contributions** RB&MG conceptualised the study, IC performed the analyses and wrote the
- 679 manuscript under the guidance of RB&MG.
- 680 Corresponding author Correspondence to Imogen Carter.
- 681 Ethics Declarations
- 682 **Conflicts of interest** The authors declare that they have no conflict of interest.

- 683 Ethics approval Not applicable.
- 684 **Consent to participate** Not applicable.
- 685 **Consent for publication** Not applicable.

## References

- Ainsworth, E.A., Rogers, A., 2007. The response of photosynthesis and stomatal conductance to rising [CO 2]: mechanisms and environmental interactions. Plant Cell&Environment 30, 258–270. https://doi.org/10.1111/j.1365-3040.2007.01641.x

  Allison, G.B., Barnes, C.J., Hughes, M.W., 1983. The distribution of deuterium and 180 in dry soils 2. Experimental. Journal of Hydrology 64, 377–397.

  https://doi.org/10.1016/0022-1694(83)90078-1
- Bader, M.K.F., Leuzinger, S., Keel, S.G., Siegwolf, R.T.W., Hagedorn, F., Schleppi,
  P.&Körner, C. 2013. Central European hardwood trees in a high-CO2 future: synthesis of an
  8-year forest canopy CO2 enrichment project. Journal of Ecology, 101, 1509-1519
- Ballantyne, A.P., Alden, C.B., Miller, J.B., Tans, P.P., White, J.W.C., 2012. Increase in observed net carbon dioxide uptake by land and oceans during the past 50 years. Nature 488, 70–72. https://doi.org/10.1038/nature11299
- Barbour, M.M., 2007. Stable oxygen isotope composition of plant tissue: a review.

  Functional Plant Biol. 34, 83. https://doi.org/10.1071/FP06228
- Barbour, M.M., Farquhar, G.D., 2000. Relative humidity- and ABA-induced variation in carbon and oxygen isotope ratios of cotton leaves. Plant Cell&Environment 23, 473–485.

  https://doi.org/10.1046/j.1365-3040.2000.00575.x

- Barbour, M.M., Fischer, R.A., Sayre, K.D., Farquhar, G.D., 2000. Oxygen isotope ratio of
- leaf and grain material correlates with stomatal conductance and grain yield in irrigated
- wheat. Functional Plant Biol. 27, 625. https://doi.org/10.1071/PP99041
- Barbour, M.M., Loucos, K.E., Lockhart, E.L., Shrestha, A., McCallum, D., Simonin, K.A.,
- Song, X., Griffani, D.S., Farquhar, G.D., 2021. Can hydraulic design explain patterns of leaf
- water isotopic enrichment in C 3 plants? Plant Cell & Environment 44, 432-444.
- 710 https://doi.org/10.1111/pce.13943
- Barbour, M.M., Roden, J.S., Farquhar, G.D., Ehleringer, J.R., 2004. Expressing leaf water
- and cellulose oxygen isotope ratios as enrichment above source water reveals evidence of a
- 713 Peclet effect. Oecologia 138, 426–435. <a href="https://doi.org/10.1007/s00442-003-1449-3">https://doi.org/10.1007/s00442-003-1449-3</a>
- Barbour, M.M., White, M.A. and Liu, L. (2024), H<sub>2</sub><sup>18</sup>O vapour labelling reveals evidence
- of radial Péclet effects, but in not all leaves. New Phytol, 244: 1263-1274.
- 716 https://doi.org/10.1111/nph.20087
- Barnard, R.L., Salmon, Y., Kodama, N., Sörgel, K., Holst, J., Rennenberg, H., Gessler, A.
- And Buchmann, N. (2007), Evaporative enrichment and time lags between  $\delta^{18}$ O of leaf water
- and organic pools in a pine stand. Plant, Cell&Environment, 30: 539-550.
- 720 https://doi.org/10.1111/j.1365-3040.2007.01654.x
- Barnard, H.R., Brooks, J.R., Bond, B.J., 2012. Applying the dual-isotope conceptual
- model to interpret physiological trends under uncontrolled conditions. Tree Physiology 32,
- 723 1183-1198. <a href="https://doi.org/10.1093/treephys/tps078">https://doi.org/10.1093/treephys/tps078</a>
- Battipaglia, G., Saurer, M., Cherubini, P., Calfapietra, C., McCarthy, H.R., Norby, R.J. and
- Francesca Cotrufo, M. 2013. Elevated CO<sub>2</sub> increases tree-level intrinsic water use efficiency:
- insights from carbon and oxygen isotope analyses in tree rings across three forest FACE sites.
- 727 *New Phytologist.* **197**(2), pp.544–554.

- Boettger, T. et al. 2007. Wood Cellulose Preparation Methods and Mass Spectrometric
- Analyses of  $\delta^{13}$ C,  $\delta^{18}$ O, and Nonexchangeable  $\delta^{2}$ H Values in Cellulose, Sugar, and Starch: An
- Interlaboratory Comparison. Analytical Chemistry 79 (12), 4603-4612. DOI:
- 731 10.1021/ac0700023
- Bottinga Y., Craig H. 1969. Oxygen isotope fractionation between CO2 and water, and
- the isotopic composition of marine atmospheric CO2. Earth and Planetary Science Letters 5,
- 734 285-295. DOI: 10.1016/S0012-821X(68)80054-8
- Buckley, T.N., 2019. How do stomata respond to water status? New Phytologist 224,
- 736 21-36. https://doi.org/10.1111/nph.15899
- Cernusak, L.A., Barbour, M.M., Arndt, S.K., Cheesman, A.W., English, N.B., Feild, T.S.,
- Helliker, B.R., Holloway-Phillips, M.M., Holtum, J.A.M., Kahmen, A., McInerney, F.A.,
- Munksgaard, N.C., Simonin, K.A., Song, X., Stuart-Williams, H., West, J.B., Farquhar, G.D., 2016.
- 540 Stable isotopes in leaf water of terrestrial plants. Plant Cell&Environment 39, 1087–1102.
- 741 https://doi.org/10.1111/pce.12703
- Cernusak, L.A., Farquhar, G.D., Pate, J.S., 2005. Environmental and physiological
- controls over oxygen and carbon isotope composition of Tasmanian blue gum, Eucalyptus
- 744 globulus. Tree Physiology 25, 129–146. https://doi.org/10.1093/treephys/25.2.129
- Cheesman, A.W., Cernusak, L.A., 2016. Infidelity in the outback: climate signal recorded
- in  $\Delta$ 18 O of leaf but not branch cellulose of eucalypts across an Australian aridity gradient.
- Tree Physiol treephys;tpw121v1. https://doi.org/10.1093/treephys/tpw121
- Craig, H., Gordon, L., 1965. Deuterium and oxygen 18 variations in the ocean and the
- marine atmosphere, in: Stable Isotopes in Oceanographic Studies and Paleotemperatures.
- Dansgaard, W., 1964. Stable isotopes in precipitation. Tellus 16, 436–468.
- 751 https://doi.org/10.1111/j.2153-3490.1964.tb00181.x

- Dawson, T.E., Ehleringer, J.R., 1991. Streamside trees that do not use stream water.
- 753 Nature 350, 335–337. https://doi.org/10.1038/350335a0
- Dongmann, G., Nürnberg, H.W., Förstel, H., Wagener, K., 1974. On the enrichment of H2
- 180 in the leaves of transpiring plants. Radiat Environ Biophys 11, 41–52.
- 756 https://doi.org/10.1007/BF01323099
- Ehleringer, J.R., Dawson, T.E., 1992. Water uptake by plants: perspectives from stable
- isotope composition. Plant Cell&Environment 15, 1073–1082.
- 759 https://doi.org/10.1111/j.1365-3040.1992.tb01657.x
- Ellison, D., Morris, C.E., Locatelli, B., Sheil, D., Cohen, J., Murdiyarso, D., Gutierrez, V.,
- Noordwijk, M.V., Creed, I.F., Pokorny, J., Gaveau, D., Spracklen, D.V., Tobella, A.B., Ilstedt, U.,
- Teuling, A.J., Gebrehiwot, S.G., Sands, D.C., Muys, B., Verbist, B., Springgay, E., Sugandi, Y.,
- Sullivan, C.A., 2017. Trees, forests and water: Cool insights for a hot world. Global
- 764 Environmental Change 43, 51–61. https://doi.org/10.1016/j.gloenvcha.2017.01.002
- Etheridge, D.M., Steele, L.P., Langenfelds, R.L., Francey, R.J., Barnola, J.-M., Morgan,
- V.I., 1996. Natural and anthropogenic changes in atmospheric CO2 over the last 1000 years
- from air in Antarctic ice and firn. J. Geophys. Res. 101, 4115–4128.
- 768 https://doi.org/10.1029/95JD03410
- Fajardo, A., Gazol, A., Mayr, C., Camarero, J.J., 2019. Recent decadal drought reverts
- varming-triggered growth enhancement in contrasting climates in the southern Andes tree
- 771 line. Journal of Biogeography 46, 1367–1379. https://doi.org/10.1111/jbi.13580
- FAO, 2024. Forests [WWW Document]. URL https://www.fao.org/forests/en
- FAO, 2020. Global Forest Resources Assessment 2020. FAO.
- 774 https://doi.org/10.4060/ca9825en

- Farquhar, G., O'Leary, M., Berry, J., 1982. On the Relationship Between Carbon Isotope
- Discrimination and the Intercellular Carbon Dioxide Concentration in Leaves. Functional Plant
- 777 Biol. 9, 121. https://doi.org/10.1071/PP9820121
- Farquhar, G.D., Lloyd, J., 1993. Carbon and Oxygen Isotope Effects in the Exchange of
- Carbon Dioxide between Terrestrial Plants and the Atmosphere, in: Stable Isotopes and Plant
- 780 Carbon-Water Relations. Elsevier, pp. 47–70.
- 781 https://doi.org/10.1016/B978-0-08-091801-3.50011-8
- Farquhar G.D., Barbour M.M., Henry B.K. 1998. Interpretation of oxygen isotope
- composition of leaf material. In 'Stable isotopes: integration of biological, ecological and
- geochemical processes'. (Ed. H Griffiths) pp. 27-61. (BIOS Scientific Publishers: Oxford)
- Feng, X., 1999. Trends in intrinsic water-use efficiency of natural trees for the past
- 100–200 years: a response to atmospheric CO2 concentration. Geochimica et Cosmochimica
- 787 Acta 63, 1891–1903. https://doi.org/10.1016/s0016-7037(99)00088-5
- Flanagan, L., Phillips, S., Ehleringer, J., Lloyd, J., Farquhar, G., 1994. Effect of Changes
- in Leaf Water Oxygen Isotopic Composition on Discrimination Against C18O16O During
- 790 Photosynthetic Gas Exchange. Functional Plant Biol. 21, 221.
- 791 https://doi.org/10.1071/PP9940221
- Frank, D.C., et al., 2015. Water-use efficiency and transpiration across European
- forests during the Anthropocene. Nature Clim Change 5, 579–583.
- 794 https://doi.org/10.1038/nclimate2614
- Gardner, A., Jiang, M., Ellsworth, D.S., MacKenzie, A.R., Pritchard, J., Bader, M.K., Barton,
- C.V.M., Bernacchi, C., Calfapietra, C., Crous, K.Y., Dusenge, M.E., Gimeno, T.E., Hall, M., Lamba,
- 797 S., Leuzinger, S., Uddling, J., Warren, J., Wallin, G., Medlyn, B.E., 2023. Optimal stomatal theory

- 798 predicts CO2 responses of stomatal conductance in both gymnosperm and angiosperm trees.
- 799 New Phytologist 237, 1229–1241. https://doi.org/10.1111/nph.18618
- Gessler A., Brandes E., Keitel C., Boda S., Kayler Z.E., Granier A., ... Treydte
- K. (2013) The oxygen isotope enrichment of leaf-exported assimilates does it always reflect
- lamina leaf water enrichment? *New Phytologist* **201**, 144–157. doi: 10.1111/nph.12359.
- GISTEMP Team. 2025. GISS Surface Temperature Analysis (GISTEMP), version 4.
- NASA Goddard Institute for Space Studies. Dataset accessed 2024-11-08.
- https://data.giss.nasa.gov/gistemp/.
- Guerrieri, R., Belmecheri, S., Ollinger, S.V., Asbjornsen, H., Jennings, K., Xiao, J., Stocker,
- 807 B.D., Martin, M., Hollinger, D.Y., Bracho-Garrillo, R., Clark, K., Dore, S., Kolb, T., Munger, J.W.,
- Novick, K., Richardson, A.D., 2019. Disentangling the role of photosynthesis and stomatal
- conductance on rising forest water-use efficiency. Proc. Natl. Acad. Sci. U.S.A. 116, 16909–
- 810 16914. https://doi.org/10.1073/pnas.1905912116
- Harris, I.C., Jones, P.D., Osborn, T. 2024. CRU TS4.08: Climatic Research Unit (CRU)
- Time-Series (TS) version 4.08 of high-resolution gridded data of month-by-month variation in
- climate (Jan. 1901- Dec. 2023). NERC EDS Centre for Environmental Data Analysis, Dataset
- 814 accessed 2024-11-08.
- 815 <a href="https://catalogue.ceda.ac.uk/uuid/715abce1604a42f396f81db83aeb2a4b/">https://catalogue.ceda.ac.uk/uuid/715abce1604a42f396f81db83aeb2a4b/</a>
- Holloway-Phillips, M., Cernusak, L. A., Barbour, M., Song, X., Cheesman, A.,
- Munksgaard, N., Stuart-Williams, H., and Farquhar, G. D. (2016) Leaf vein fraction influences
- the Péclet effect and <sup>18</sup>O enrichment in leaf water. *Plant, Cell&Environment*, 39: 2414–2427.
- 819 doi: 10.1111/pce.12792.

- Jarvis, P.G., 1976. The interpretation of the variations in leaf water potential and stomatal conductance found in canopies in the field. Phil. Trans. R. Soc. Lond. B 273, 593–
- 822 610. https://doi.org/10.1098/rstb.1976.0035
- Kahmen, A., Sachse, D., Arndt, S.K., Tu, K.P., Farrington, H., Vitousek, P.M., Dawson, T.E.,
- 824 2011. Cellulose δ 18 O is an index of leaf-to-air vapor pressure difference (VPD) in tropical
- 925 plants. Proc. Natl. Acad. Sci. U.S.A. 108, 1981–1986.
- 826 https://doi.org/10.1073/pnas.1018906108
- Kahmen, A., Simonin, K., Tu, K., Goldsmith, G.R., Dawson, T.E., 2009. The influence of species and growing conditions on the 18-O enrichment of leaf water and its impact on 'effective path length.' New Phytologist 184, 619–630.
- 830 https://doi.org/10.1111/j.1469-8137.2009.03008.x
- Keel S.G., Pepin S., Leuzinger S.&Koerner C. 2007. Stomatal conductance in mature deciduous forest trees exposed to elevated CO2. Trees- Structure and Function, 21, 151-159.
- Keeling, C.D., Bacastow, R.B., Bainbridge, A.E., Ekdahl, C.A., Guenther, P.R., Waterman,
- L.S., Chin, J.F.S., 1976. Atmospheric carbon dioxide variations at Mauna Loa Observatory,
- 835 Hawaii. Tellus 28, 538-551. https://doi.org/10.1111/j.2153-3490.1976.tb00701.x
- Keenan, T.F., Hollinger, D.Y., Bohrer, G., Dragoni, D., Munger, J.W., Schmid, H.P.,
- Richardson, A.D., 2013. Increase in forest water-use efficiency as atmospheric carbon dioxide
- 838 concentrations rise. Nature 499, 324–327. <a href="https://doi.org/10.1038/nature12291">https://doi.org/10.1038/nature12291</a>
- Klein T., Bader M.K.F., Leuzinger S., Mildner M., Schleppi P., Siegwolf R.T.W. & Korner
- 840 C. 2016. Growth and carbon relations of mature Picea abies trees under 5years of free-air CO2
- enrichment. Journal of Ecology, 104, 1720-1733.
- Lammertsma, E.I., Boer, H.J.D., Dekker, S.C., Dilcher, D.L., Lotter, A.F., Wagner-Cremer,
- F., 2011. Global CO2 rise leads to reduced maximum stomatal conductance in Florida

- vegetation. Proc. Natl. Acad. Sci. U.S.A. 108, 4035-4040.
- 845 https://doi.org/10.1073/pnas.1100371108
- Li, Y., 2024. Climate feedback from plant physiological responses to increasing
- atmospheric CO2 in Earth system models. New Phytologist 244, 2176–2182.
- 848 https://doi.org/10.1111/nph.20184
- Liang, X., Wang, D., Ye, Q., Zhang, J., Liu, M., Liu, H., Yu, K., Wang, Y., Hou, E., Zhong, B.,
- 850 Xu, L., Lv, T., Peng, S., Lu, H., Sicard, P., Anav, A., Ellsworth, D.S., 2023. Stomatal responses of
- terrestrial plants to global change. Nat Commun 14, 2188.
- 852 https://doi.org/10.1038/s41467-023-37934-7
- Lin, W., Barbour, M.M., Song, X., 2022. Do changes in tree-ring δ 18 O indicate changes
- in stomatal conductance? New Phytologist 236, 803-808. https://doi.org/10.1111/nph.18431
- Malhi, Y., Meir, P., Brown, S., 2002. Forests, carbon and global climate. Philosophical
- 856 Transactions of the Royal Society of London. Series A: Mathematical, Physical and
- 857 Engineering Sciences 360, 1567–1591. <a href="https://doi.org/10.1098/rsta.2002.1020">https://doi.org/10.1098/rsta.2002.1020</a>
- Marchin, R. M., Broadhead, A. A., Bostic, L. E., Dunn, R. R., and Hoffmann, W. A. 2016.
- Stomatal acclimation to vapour pressure deficit doubles transpiration of small tree seedlings
- with warming. Plant, Cell & Environment, 39: 2221–2234. doi: 10.1111/pce.12790.
- Mathias, J.M., Thomas, R.B., 2021. Global tree intrinsic water use efficiency is
- enhanced by increased atmospheric CO 2 and modulated by climate and plant functional
- types. Proc. Natl. Acad. Sci. U.S.A. 118, e2014286118.
- 864 <a href="https://doi.org/10.1073/pnas.2014286118">https://doi.org/10.1073/pnas.2014286118</a>
- McDowell, N., Pockman, W.T., Allen, C.D., Breshears, D.D., Cobb, N., Kolb, T., Plaut, J.,
- Sperry, J., West, A., Williams, D.G. and Yepez, E.A. 2008. Mechanisms of plant survival and

mortality during drought: why do some plants survive while others succumb to drought?. New Phytologist, 178: 719-739.

Medlyn, B.E., Barton, C.V.M., Broadmeadow, M.S.J., Ceulemans, R., De Angelis, P.,
Forstreuter, M., Freeman, M., Jackson, S.B., Kellomäki, S., Laitat, E., Rey, A., Roberntz, P.,
Sigurdsson, B.D., Strassemeyer, J., Wang, K., Curtis, P.S., Jarvis, P.G., 2001. Stomatal
conductance of forest species after long-term exposure to elevated CO 2 concentration: a
synthesis. New Phytologist 149, 247–264. https://doi.org/10.1046/j.1469-8137.2001.00028.x

Moreno-Gutiérrez, C., Dawson, T.E., Nicolás, E., Querejeta, J.I., 2012. Isotopes reveal

Moreno-Gutiérrez, C., Dawson, T.E., Nicolás, E., Querejeta, J.I., 2012. Isotopes reveal contrasting water use strategies among coexisting plant species in a Mediterranean ecosystem. New Phytologist 196, 489–496.

https://doi.org/10.1111/j.1469-8137.2012.04276.x

Morgner, E., Holloway-Phillips, M., Basler, D., Nelson, D.B., Kahmen, A., 2024. Effects of increasing atmospheric CO2 on leaf water  $\delta18$  O values are small and are attenuated in grasses and amplified in dicotyledonous herbs and legumes when transferred to cellulose  $\delta18$  O values. New Phytologist 242, 1944–1956. https://doi.org/10.1111/nph.19713

Nock, C.A., Baker, P.J., Wanek, W., Leis, A., Grabner, M., Bunyavejchewin, S., Hietz, P., 2011. Long-term increases in intrinsic water-use efficiency do not lead to increased stem growth in a tropical monsoon forest in western Thailand. Global Change Biology 17, 1049–1063. https://doi.org/10.1111/j.1365-2486.2010.02222.x

Norby, R.J., Wullschleger, S.D., Gunderson, C.A., Johnson, D.W., Ceulemans, R., 1999. Tree responses to rising CO 2 in field experiments: implications for the future forest. Plant Cell&Environment 22, 683–714. https://doi.org/10.1046/j.1365-3040.1999.00391.x

Norby, R.J., Zak, D.R., 2011. Ecological Lessons from Free-Air CO2 Enrichment (FACE) 889 Experiments. Annu. Rev. Ecol. Evol. Syst. 42, 181-203. 890 https://doi.org/10.1146/annurev-ecolsys-102209-144647 891 Osmond, C.B., Björkman, O., Anderson, D.J., 1980. Physiological Processes in Plant 892 Ecology, Ecological Studies. Springer Berlin Heidelberg, Berlin, Heidelberg. 893 https://doi.org/10.1007/978-3-642-67637-6 894 Pan, Y., Birdsey, R.A., Phillips, O.L., Houghton, R.A., Fang, J., Kauppi, P.E., Keith, H., Kurz, 895 W.A., Ito, A., Lewis, S.L., Nabuurs, G.-J., Shvidenko, A., Hashimoto, S., Lerink, B., 896 Schepaschenko, D., Castanho, A., Murdiyarso, D., 2024. The enduring world forest carbon sink. 897 Nature 631, 563-569. https://doi.org/10.1038/s41586-024-07602-x 898 Parmesan, C., Hanley, M.E., 2015. Plants and climate change: complexities and 899 surprises. Annals of Botany 116, 849-864. https://doi.org/10.1093/aob/mcv169 900 Roden, J., Siegwolf, R., 2012. Is the dual-isotope conceptual model fully operational? 901 Tree Physiology 32, 1179-1182. <a href="https://doi.org/10.1093/treephys/tps099">https://doi.org/10.1093/treephys/tps099</a> 902 Roden, J., Kahmen, A., Buchmann, N., and Siegwolf, R. (2015) The enigma of effective 903 path length for <sup>18</sup>O enrichment in leaf water of conifers. *Plant Cell Environ*, 38: 2551–2565. 904 doi: 10.1111/pce.12568. 905 Roden JS, Ehleringer JR. Observations of hydrogen and oxygen isotopes in leaf water 906 confirm the Craig-Gordon model under wide-ranging environmental conditions. Plant Physiol. 907 1999 Aug;120(4):1165-74. doi: 10.1104/pp.120.4.1165. PMID: 10444100; PMCID: PMC59350. 908 Roden, J.S., Lin, G., Ehleringer, J.R., 2000. A mechanistic model for interpretation of 909 hydrogen and oxygen isotope ratios in tree-ring cellulose. Geochimica et Cosmochimica Acta 910 64, 21-35. <a href="https://doi.org/10.1016/S0016-7037(99)00195-7">https://doi.org/10.1016/S0016-7037(99)00195-7</a> 911

912 Roden, J., Saurer, M., and Siegwolf, R.T.W. 2022. Probing Tree Physiology Using the Dual-Isotope Approach. In: Siegwolf, R.T.W., Brooks, J.R., Roden, J., Saurer, M. (eds) Stable 913 Isotopes in Tree Rings. Tree Physiology, vol 8. Springer, Cham. 914 doi.org/10.1007/978-3-030-92698-4\_16Rozanski, K., Araguás-Araguás, L., Gonfiantini, R., 915 1992. Relation Between Long-Term Trends of Oxygen-18 Isotope Composition of Precipitation 916 and Climate. Science 258, 981-985. https://doi.org/10.1126/science.258.5084.981 917 Saurer, M., Siegwolf, R.T.W., Schweingruber, F.H., 2004. Carbon isotope discrimination 918 indicates improving water-use efficiency of trees in northern Eurasia over the last 100 years. 919 Global Change Biology 10, 2109-2120. https://doi.org/10.1111/j.1365-2486.2004.00869.x 920 Scheidegger, Y., Saurer, M., Bahn, M., Siegwolf, R., 2000. Linking stable oxygen and 921 carbon isotopes with stomatal conductance and photosynthetic capacity: a conceptual 922 model. Oecologia 125, 350-357. https://doi.org/10.1007/s004420000466 923 Schimel, D., Stephens, B.B., Fisher, J.B., 2015. Effect of increasing CO2 on the 924 terrestrial carbon cycle. Proc. Natl. Acad. Sci. U.S.A. 112, 436-441. 925 https://doi.org/10.1073/pnas.1407302112 926 Siegwolf, R.T.W., Lehmann, M.M., Goldsmith, G.R., Churakova (Sidorova), O.V., Mirande-927 Ney, C., Timoveeva, G., Weigt, R.B., Saurer, M., 2023. Updating the dual C and O isotope—Gas-928 exchange model: A concept to understand plant responses to the environment and its 929 implications for tree rings. Plant Cell&Environment 46, 2606–2627. 930 https://doi.org/10.1111/pce.14630 931 Song, X., Barbour, M.M., Farquhar, G.D., Vann, D.R., Helliker, B.R., 2013. Transpiration 932

rate relates to within- and across-species variations in effective path length in a leaf water
model of oxygen isotope enrichment. Plant Cell & Environment 36, 1338–1351. DOI:
10.1111/pce.12063

Song X, Clark KS, Helliker BR. 2014. Interpreting species-specific variation in tree-ring oxygen isotope ratios among three temperate forest trees. *Plant, Cell& Environment* **37**: 2169–938 2183.

Sprenger, M., Tetzlaff, D., Soulsby, C., 2017. Soil water stable isotopes reveal evaporation dynamics at the soil-plant-atmosphere interface of the critical zone. Hydrol. Earth Syst. Sci. 21, 3839–3858. DOI: 10.5194/hess-21-3839-2017

Sternberg, L., Ellsworth, P.F.V., 2011. Divergent Biochemical Fractionation, Not Convergent Temperature, Explains Cellulose Oxygen Isotope Enrichment across Latitudes. PLoS ONE 6, e28040. https://doi.org/10.1371/journal.pone.0028040

Sternberg L. S. L., Pinzon M. C., Vendramini P. F., Anderson W. T., Jahren A. H. and Beuning K. 2007. Oxygen isotope ratios of cellulose-derived phenylglucosazone: an improved paleoclimate indicator of environmental water and relative humidity. Geochim. Cosmochim. Acta 71, 2463–2473

Sternberg, L.D.S.L., Anderson, W.T., Morrison, K., 2003. Separating soil and leaf water 180 isotopic signals in plant stem cellulose. Geochimica et Cosmochimica Acta 67, 2561–2566. https://doi.org/10.1016/S0016-7037(03)00109-1

Sternberg, L.D.S.L., Deniro, M.J., Savidge, R.A., 1986. Oxygen Isotope Exchange between Metabolites and Water during Biochemical Reactions Leading to Cellulose Synthesis. Plant Physiol. 82, 423–427. https://doi.org/10.1104/pp.82.2.423

Stewart, J.B., 1988. Modelling surface conductance of pine forest. Agricultural and Forest Meteorology 43, 19–35. <a href="https://doi.org/10.1016/0168-1923(88)90003-2">https://doi.org/10.1016/0168-1923(88)90003-2</a>

Streit K., Siegwolf R.T.W., Hagedorn F., Schaub M. & Buchmann N. 2014. Lack of photosynthetic or stomatal regulation after 9 years of elevated CO2 and 4 years of soil warming in two conifer species at the alpine treeline. Plant Cell and Environment, 37, 315-326.

- Sullivan, P.F., Welker, J.M., 2007. Variation in leaf physiology of Salix arctica within and across ecosystems in the High Arctic: test of a dual isotope (Δ13C and Δ18O) conceptual model. Oecologia 151, 372. https://doi.org/10.1007/s00442-006-0602-1
- Tardieu, F., and Simonneau, T. 1998. Variability among species of stomatal control under fluctuating soil water status and evaporative demand: modelling isohydric and anisohydric behaviours. Journal of Experimental Botany, 49, 419–432.
- Treydte, K., Liu, L., Padrón, R.S. *et al.* 2023. Recent human-induced atmospheric drying across Europe unprecedented in the last 400 years. *Nat. Geosci.* **17**, 58–65.
- 968 https://doi.org/10.1038/s41561-023-01335-8
- Urban, J., Ingwers, M., McGuire, M.A., Teskey, R.O., 2017. Stomatal conductance increases with rising temperature. Plant Signaling & Behavior 12, e1356534.
- 971 https://doi.org/10.1080/15592324.2017.1356534
- Van Der Ent, R.J., Savenije, H.H.G., Schaefli, B., Steele-Dunne, S.C., 2010. Origin and fate of atmospheric moisture over continents. Water Resources Research 46, 2010WR009127.
- 974 https://doi.org/10.1029/2010WR009127
- Van Der Sleen, P., Groenendijk, P., Vlam, M., Anten, N.P.R., Boom, A., Bongers, F., Pons,
- 976 T.L., Terburg, G., Zuidema, P.A., 2015. No growth stimulation of tropical trees by 150 years of
- 977 CO2 fertilization but water-use efficiency increased. Nature Geosci 8, 24–28.
- 978 https://doi.org/10.1038/ngeo2313
- Walker, A.P., et al. 2021 Integrating the evidence for a terrestrial carbon sink caused by increasing atmospheric CO2. New Phytologist 229, 2413–2445.
- 981 https://doi.org/10.1111/nph.16866

982 Walker, C.D., Leaney, F.W., Dighton, J.C., Allison, G.B., 1989. The influence of transpiration on the equilibration of leaf water with atmospheric water vapour. Plant 983 Cell&Environment 12, 221–234. DOI: <u>10.1111/j.1365-3040.1989.tb01937.x</u> 984 985 Wang X.F., Yakir D. & Avishai M. (1998) Non-climatic variations in the oxygen isotopic composition of plants. Global Change Biology 4, 835-849. 986 Waterhouse, J.S., Cheng, S., Juchelka, D., Loader, N.J., McCarroll, D., Switsur, V.R., 987 Gautam, L., 2013. Position-specific measurement of oxygen isotope ratios in cellulose: 988 Isotopic exchange during heterotrophic cellulose synthesis. Geochimica et Cosmochimica 989 Acta 112, 178–191. https://doi.org/10.1016/j.gca.2013.02.021 990 Zweiniecki M.A., Brodribb T.J. & Holbrook N. (2007) Hydraulic design of leaves: 991 insights from rehydration kinetics. *Plant, Cell&Environment* **30**, 910–921. 992 doi: 10.1111/j.1365-3040.2007.001681.x. 993